



NATIONAL CENTER FOR EARTHQUAKE  
ENGINEERING RESEARCH

State University of New York at Buffalo

TWO HYBRID CONTROL SYSTEMS  
FOR BUILDING STRUCTURES  
UNDER STRONG EARTHQUAKES

by

J. N. Yang and A. Danielians  
Department of Civil, Mechanical and Environmental Engineering  
The George Washington University  
Washington, D.C. 20052

Technical Report NCEER-90-0015

June 29, 1990

This research was conducted at The George Washington University and was partially supported by the National Science Foundation under Grant No. ECE 86-07591.

## NOTICE

This report was prepared by The George Washington University as a result of research sponsored by the National Center for Earthquake Engineering Research (NCEER) and the National Science Foundation. Neither NCEER, associates of NCEER, its sponsors, The George Washington University, nor any person acting on their behalf:

- a. makes any warranty, express or implied, with respect to the use of any information, apparatus, method, or process disclosed in this report or that such use may not infringe upon privately owned rights; or
- b. assumes any liabilities of whatsoever kind with respect to the use of, or the damage resulting from the use of, any information, apparatus, method or process disclosed in this report.



TWO HYBRID CONTROL SYSTEMS FOR BUILDING  
STRUCTURES UNDER STRONG EARTHQUAKES

by

J.N. Yang<sup>1</sup> and A. Danielians<sup>2</sup>

June 29, 1990

Technical Report NCEER-90-0015

NCEER Project Number 89-2202 and NSF Grant Number BCS-89-04524

NSF Master Contract Number ECE 86-07591

- 1 Professor, Department of Civil, Mechanical and Environmental Engineering, George Washington University
- 2 Graduate Research Assistant, Department of Civil, Mechanical and Environmental Engineering, George Washington University

NATIONAL CENTER FOR EARTHQUAKE ENGINEERING RESEARCH  
State University of New York at Buffalo  
Red Jacket Quadrangle, Buffalo, NY 14261



## PREFACE

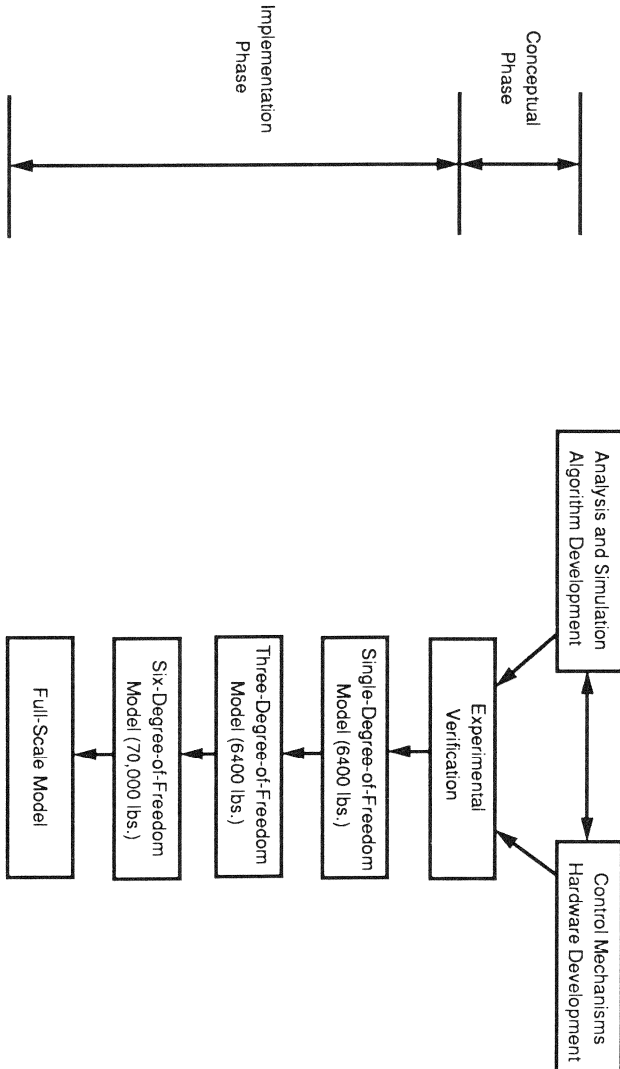
The National Center for Earthquake Engineering Research (NCEER) is devoted to the expansion and dissemination of knowledge about earthquakes, the improvement of earthquake-resistant design, and the implementation of seismic hazard mitigation procedures to minimize loss of lives and property. The emphasis is on structures and lifelines that are found in zones of moderate to high seismicity throughout the United States.

NCEER's research is being carried out in an integrated and coordinated manner following a structured program. The current research program comprises four main areas:

- Existing and New Structures
- Secondary and Protective Systems
  - Lifeline Systems
- Disaster Research and Planning

This technical report pertains to Program 2, Secondary and Protective Systems, and more specifically, to protective systems. Protective Systems are devices or systems which, when incorporated into a structure, help to improve the structure's ability to withstand seismic or other environmental loads. These systems can be passive, such as base isolators or viscoelastic dampers; or active, such as active tendons or active mass dampers; or combined passive-active systems.

In the area of active systems, research has progressed from the conceptual phase to the implementation phase with emphasis on experimental verification. As the accompanying figure shows, the experimental verification process began with a small single-degree-of-freedom structure model, moving to larger and more complex models, and finally, to full-scale models.



*In the general research area of protective systems, passive systems, such as base isolation systems, and active systems, such as active mass dampers and tendon systems, have largely been considered separately. Both types of the protective systems have their strengths as well as inherent weaknesses. It is the purpose of this report to explore the merit of hybrid systems which combine passive and active systems in order to capitalize on their strengths while minimizing their weaknesses. The hybrid system considered in this report consists of a base isolation system coupled with either a passive or an active mass damper. The performance of this system is investigated under simulated seismic conditions and it is shown that it can be effective in response reduction of either high-rise or low-rise buildings under strong earthquakes.*

## ABSTRACT

Two aseismic hybrid control systems are proposed for protecting building structures against strong earthquakes. The hybrid control system consists of a base isolation system connected to either a passive or active mass damper. The base isolation system, such as elastomeric bearings, is used to decouple the horizontal ground motions from the building, whereas the mass damper, either active or passive, is used to protect the safety and integrity of the base isolation system. The performance of the proposed hybrid control systems is investigated, evaluated, and compared with that of an active control system. It is shown from the theoretical/numerical results that the proposed hybrid control systems are very effective in reducing the response of either high-rise or low-rise buildings under strong earthquakes. Likewise, the practical implementation of such hybrid control systems is easier than that of an active control system alone.



ACKNOWLEDGMENT

This research effort is partially supported by the National Center for Earthquake Engineering Research Grant No. NCEER-89-2202 and National Science Foundation Grant No. NSF-BCS-89-04524.



TABLE OF CONTENTS

SECTION	TITLE	PAGE
1	INTRODUCTION . . . . .	1-1
2	FORMULATION . . . . .	2-1
3	NUMERICAL ANALYSIS . . . . .	3-1
3.1	Example 1: A Twenty-Story Building . . . . .	3-1
3.2	Example 2: A Laboratory Scaled Five-Story Building.	3-19
4	CONCLUSIONS . . . . .	4-1
5	REFERENCES . . . . .	5-1



LIST OF FIGURES

FIGURE	TITLE	PAGE
2-1	A Multi-Story Building Model With Aseismic Hybrid Control System; (a) Passive Hybrid Control System, and (b) Active Hybrid Control System . . . . .	2-2
2-2	A Multi-Story Building Model With Control System; (a) An Active Mass Damper, and (b) A Base Isolation System . . . . .	2-3
3-1	A Simulated Earthquake Ground Acceleration . . . . .	3-2
3-2	Deformation of First Story Unit: (a) Building Without Control; (b) With Base Isolation System; (c) With Passive Hybrid Control System ( $m_d = 100\% m_i$ ); (d) With Active Hybrid Control System (Control Force = 1031 kN); (e) With Active Control System (Control Force = 1102 kN).	3-3
3-3	Deformation of Base Isolation System: (a) Without Mass Damper; (b) With Passive Mass Damper ( $m_d = 100\% m_i$ ); (c) With Active Mass Damper (Control Force = 1031 kN) . . . . .	3-6
3-4	Maximum Deformation of First Story Unit and Base Isolation System as Function of Mass Ratio of Passive Damper: (1) Base Isolation System Without P-Delta Effect; (2) Base Isolation System With P-Delta Effect; (3) First Story Unit Without P-Delta Effect; (4) First Story Unit With P-Delta Effect . . . . .	3-8
3-5	Maximum Deformation of Base Isolation System and Maximum Control Force as Function of $\alpha/R$ : (1) Base Isolation System Without P-Delta Effect; (2) Control Force Without P-Delta Effect; (3) Base Isolation System With P-Delta Effect; (4) Control Force With P-Delta Effect . . . . .	3-13
3-6	Maximum Displacement of The Top Floor Relative to The Base and Maximum Control Force as Function of $\alpha/R$ : (1) Top Floor Displacement Without P-Delta Effect; (2) Control Force Without P-Delta Effect; (3) Top Floor Displacement with P-Delta Effect; (4) Control Force With P-Delta Effect . . . . .	3-14
3-7	Maximum Displacement of The Structural System With Respect to The Ground: (1) Without Control; (2) Base Isolation System Without P-Delta Effect; (3) Passive Hybrid Control System Without P-Delta Effect (Mass Ratio 100%); (4) Active Hybrid Control System Without P-Delta Effect; (5) Base Isolation System With P-Delta Effect;	

LIST OF FIGURES (Continued)

FIGURE NUMBER	TITLE	PAGE
	(6) Passive Hybrid Control System With P-Delta Effect; (7) Active Hybrid Control System With P-Delta Effect . . . . .	3-15
3-8	<b>Maximum Deformation of First Story Unit and Maximum Control Force as Function of <math>\alpha/R</math> (Active Mass Damper on Top Floor) . . . . .</b>	3-18
3-9	Deformation of First Story Unit: (a) Building Without Control; (b) With Base Isolation System; (c) With Passive Hybrid Control System ( $m_d=20\% m_i$ ); (d) With Active Hybrid Control System ( $m_d=10\% m_i$ and $\alpha/R=30$ ) . . . . .	3-22
3-10	Deformation of Base Isolation System: (a) Without Mass Damper; (b) With Passive Mass Damper $m_d=10\% m_i$ ; (c) $m_d=20\% m_i$ ; (d) $m_d=30\% m_i$ ; (e) With Active Mass Damper ( $m_d=10\% m_i$ , $\alpha/R = 30$ ) . . . . .	3-24
3-11	Maximum Deformation of Base Isolation System as a Function of mass ratio $\gamma = m_d/m_i$ . . . . .	3-26
3-12	Required Active Control Force With $m_d=10\% m_i$ and $\alpha/R=30$ . . . . .	3-29
3-13	<b>Maximum Deformation of Base Isolation System and Maximum Control Force as a Function of <math>\alpha/R</math> . . . . .</b>	3-31
3-14	Maximum Deformation of First Story Unit and Maximum Control Force as A Function of $\alpha/R$ (Active Mass Damper on Top Floor) . . . . .	3-34
3-15	Maximum Displacement of The Building System: (1) Without Control; (2) With Base Isolation System; (3) With Passive Hybrid Control System $m_d=10\% m_i$ ; (4) With Passive Hybrid Control System $m_d=20\% m_i$ ; (5) With Passive Hybrid Control System $m_d=30\% m_i$ ; (6) With Active Hybrid Control System $m_d=10\% m_i$ ; (7) With Active Mass Damper On Top Floor $m_d=10\% m_i$ . . . . .	3-35

LIST OF TABLES

TABLE	TITLE	PAGE
3-II	Maximum Structural Response: Passive Hybrid Control System . . . . .	3-4
3-III	Maximum Structural Response: Active Hybrid Control System . . . . .	3-11
3-IV	Maximum Structural Response: Active Mass Damper Alone . . . . .	3-17
3-V	Maximum Structural Response: (Five-Story Model) Passive Hybrid Control System . . . . .	3-21
3-VI	Maximum Structural Response: (Five-Story Model) Active Hybrid Control System . . . . .	3-30
	Maximum Structural Response: (Five-Story Model) Active Mass Damper Alone . . . . .	3-33



SECTION 1  
INTRODUCTION

In recent years, considerable progress has been made in the area of aseismic protective systems for civil engineering structures. Aseismic protective systems, in general, consist of two categories; namely, passive protective systems and active protective systems. The active protective system differs from the passive one in that it requires the supply of external power to counter the motion of the structure to be protected.

The application of active control systems to building structures which are subjected to strong earthquakes and other natural hazards has become an area of considerable interest both theoretically and experimentally in recent years. A literature review of recent advancement in active control of civil engineering structures was made by Yang and Soong [16], Reinhorn and Manolis [5], and Soong [10]. Since the pioneer works of Yao [20], significant progress has been made in active control of civil engineering structures.

The horizontal components of the earthquake ground motions are the most damaging to the building. An important class of passive aseismic protective systems is the base isolation system, which is able to reduce the horizontal seismic forces transmitted to the structure. Excellent literature reviews in this area were presented, for instance, by Kelly [3] and Constantinou and Reinhorn [2]. Extensive theoretical and experimental research has been carried out on the lead-rubber bearing systems. The lead-rubber bearings have the mechanical characteristics of being flexible in the horizontal direction and stiff in the vertical direction. The purpose of this isolation

system is to lower the fundamental frequency of the entire structural system to be outside the range of frequencies which dominate the earthquake excitation.

While passive base isolation systems are effective for protecting seismic-excited buildings, there are limitations. Passive systems are limited to low-rise buildings, because for tall buildings, uplift forces may be generated in the isolation system leading to an instability failure. Furthermore, in some base isolation systems, such as lead-core elastomeric bearings, inelastic or permanent deformation may accumulate after each earthquake episode. Thus, the passive protective system alone is not sufficiently proven for the protection of seismic-excited tall buildings.

On the other hand, when an active control system is used alone as a primary aseismic protective system for tall buildings, the required active control force and force rate to be provided by the external power source may be very large. Hence, a large or powerful active control system may be needed. For the installation of a large active control system with large stand-by energy sources, the issues of cost, reliability and practicality remain to be resolved.

The purpose of this report is to study the feasibility of the hybrid control concept and to specifically propose two types of hybrid control systems for seismic-excited tall buildings. These hybrid systems consist of a base isolation system, such as elastomeric bearings, connected to either passive or active mass dampers. With such hybrid systems, the advantage of the base isolation system, whose ability to drastically reduce the horizontal motion

of the building, is preserved, whereas its safety and integrity are protected by either the passive or active mass damper. The idea of such aseismic hybrid control systems was suggested by Yang, et al. [17-19]. Other types of hybrid protective systems have also been considered recently [e.g., 4,6,7]. The performance of these two hybrid control systems is evaluated and compared with that of an active control system for a twenty-story building and a five-story building model subjected to a strong earthquake. It is shown that the proposed hybrid control systems are very effective in reducing the response of building structures under strong earthquake excitations and that they may be more effective and advantageous than the application of an active control system alone.

Under strong earthquake excitations, tall buildings may undergo significant lateral displacements. During a lateral motion, the gravitational load of the building results in an overturning moment. The effect of such an overturning moment is referred to as the P-delta effect [e.g., 1,9,11], since the overturning moment is approximately equal to the weight "P" of the building multiplied by the lateral displacement "delta". For well designed building structures with small lateral displacement under seismic loads, the P-delta effect is usually of the second order and it may be negligible. However, for buildings implemented by a base isolation system, the lateral displacement of the base isolation system may be significant and hence the P-delta effect may be important.

The P-delta effect on the dynamic response of buildings implemented by two types of hybrid control systems proposed herein; namely, passive and active hybrid control systems, is also investigated. It is shown that the P-delta

effect should be accounted for in the analysis of building structures implemented by the proposed hybrid control systems.

SECTION 2  
FORMULATION

Consider a base-isolated shear-beam building structure implemented by an active mass damper as shown in Fig. 2-1(b). The structural system is idealized by an  $n + 2$  (including the base isolation system and the mass damper) degrees of freedom system and subjected to a one-dimensional earthquake ground acceleration  $\ddot{x}_0(t)$ . The matrix equation of motion of the entire structural system can be written as

$$\underline{M} \ddot{\underline{Y}}(t) + \underline{C} \dot{\underline{Y}}(t) + \underline{K} \underline{Y}(t) = -\underline{M} \underline{\nu} \ddot{x}_0(t) + \underline{H} \underline{U}(t) \quad (2.1)$$

in which the quantity with an under-bar denotes either a vector or a matrix;  $\underline{Y}(t) = [y_d, y_b, y_1, \dots, y_n]'$  = a  $(n+2)$  response vector, where a prime ' indicates the transpose of a vector or matrix;  $y_i$  = relative displacement of the  $i$ th floor with respect to the ground;  $y_d$  and  $y_b$  are relative displacements of the mass damper and the base isolation system, respectively, with respect to the ground;  $\underline{\nu} = [1, 1, 1, \dots, 1]'$  = a  $(n+2)$  unit vector;  $\underline{H} = [-1, 0, 0, \dots, 0]'$  = a  $(n+2)$  vector with a non-zero element; and  $\underline{U}(t)$  is the active control force vector. In Eq. (2.1),  $\underline{M}$  = a  $(n+2) \times (n+2)$  diagonal mass matrix with the diagonal elements  $m_{1,1} = m_d$  = mass of the mass damper,  $m_{2,2} = m_b$  = mass of the base isolation system,  $m_{i+2,i+2} = m_i$  = mass of the  $i$ th floor ( $i = 1, 2, \dots, n$ ).  $\underline{C}$  and  $\underline{K}$  are  $(n+2) \times (n+2)$  damping and stiffness matrices, respectively. If the mass damper is passive, Fig. 2-1(a),  $\underline{H} = 0$  and  $\underline{U}(t) = 0$ . For the building implemented by an active mass damper on the top floor alone as shown in Fig. 2-2(a), the number of degrees of freedom is  $n+1$ .

The axial force at a story level, which is the sum of the structural weight

2-2

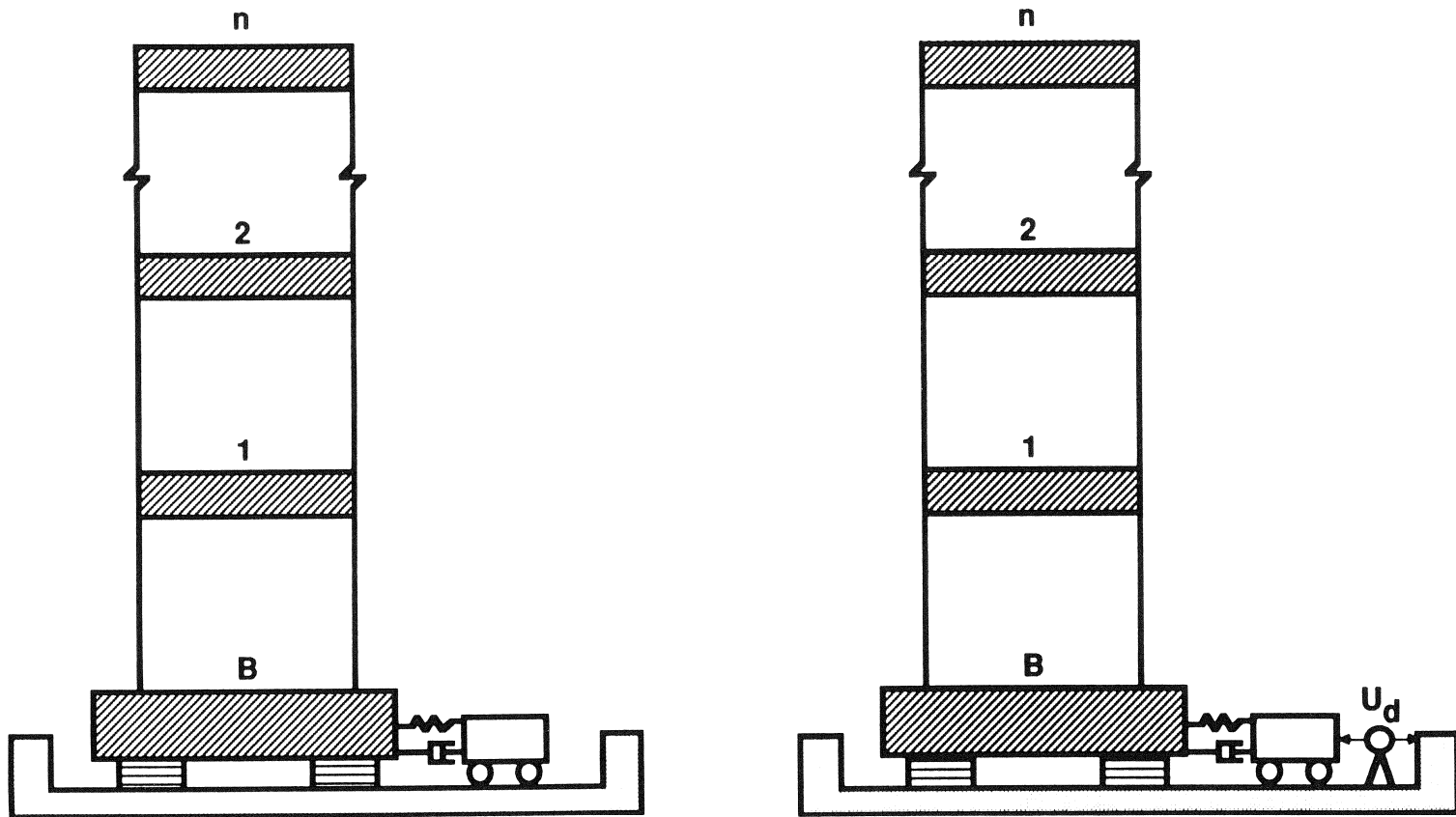


Figure 2-1: A Multi-Story Building Model With Aseismic Hybrid Control System; (a) Passive Hybrid Control System, and (b) Active Hybrid Control System.

2-3

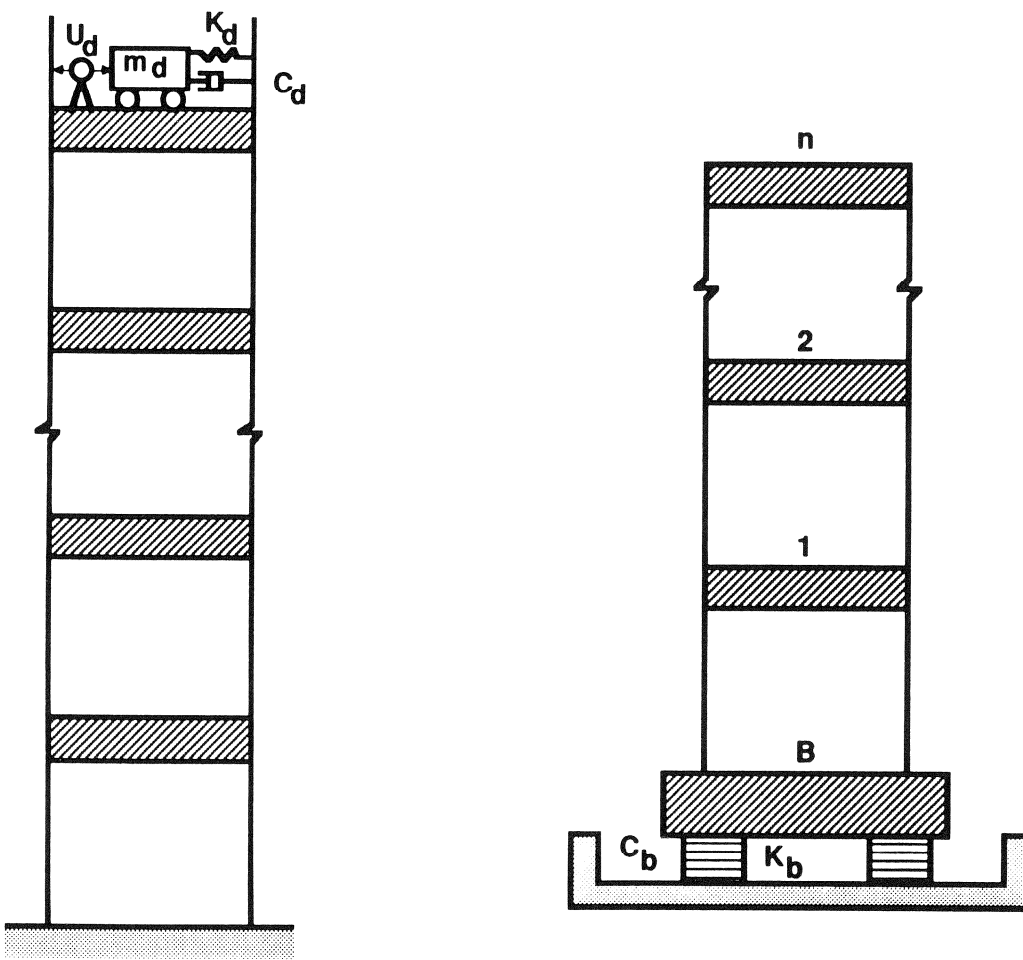


Figure 2-2: A Multi-Story Building Model With Control System; (a) An Active Mass Damper, and (b) A Base Isolation System.

above that level, is assumed to be constant during the earthquake-excited motion. The P-delta effect is taken into account by a constant geometric stiffness matrix  $\underline{K}_G$ , i.e.,

$$\underline{K} = \underline{K}_e - \underline{K}_G \quad (2.2)$$

where  $\underline{K}_e$  is the elastic stiffness matrix and  $\underline{K}_G$  is the geometric stiffness matrix [e.g., 9,11,18]. The geometric stiffness matrix  $\underline{K}_G$  and the stiffness of the rubber bearing with and without the P-delta effect are described in the following.

The additional overturning moment applied to the  $i$ th story unit, denoted by  $M_i^*$ , resulting from the axial force,  $P_i$ , that is the total weight above and including the  $i$ th story, is given by [e.g., 9,11]

$$M_i^* = P_i (y_i - y_{i-1}) \quad (2.3)$$

in which

$$P_i = \sum_{j=i}^n m_j g \quad (2.4)$$

To balance such an additional moment  $M_i^*$ , an equivalent lateral force  $V_i$  should be applied to the upper and lower ends of the  $i$ th story unit; with the results [e.g., 9]

$$V_i = M_i^* / h_i = P_i (y_i - y_{i-1}) / h_i \quad (2.5)$$

where  $h_i$  is the height of the  $i$ th story unit. This approximation is made by assuming that both the upper and lower ends of the columns of the  $i$ th story

unit are free to rotate (hinged-ends). In the formulation for the equations of motion, Eq. (2.1), however, the rotation of both ends of the columns was assumed to be zero. With the fixed-ended boundary conditions, the equivalent lateral force  $v_i$  can be computed from  $M_i^*$  in terms of transcendental functions. It can be shown, however, that the hinged-ends approximation is conservative and reasonable, and it has been used extensively in the literature [e.g., 9,11].

The equivalent additional lateral forces applied to all floor masses of the structure, except the foundation  $m_b$  and the mass damper  $m_d$ , can be casted into a matrix form as

$$\begin{bmatrix} v_1 \\ v_2 \\ \vdots \\ v_i \\ \vdots \\ v_n \end{bmatrix} = \begin{bmatrix} \frac{P_1}{h_1} + \frac{P_2}{h_2} & -\frac{P_2}{h_2} & 0 & & & \\ -\frac{P_2}{h_2} & \frac{P_2}{h_2} + \frac{P_3}{h_3} & -\frac{P_3}{h_3} & & & \\ \vdots & & & & & \\ -\frac{P_i}{h_i} & \frac{P_i}{h_i} + \frac{P_{i+1}}{h_{i+1}} & -\frac{P_{i+1}}{h_{i+1}} & y_i & \cdot & \\ \vdots & & & & & \\ -\frac{P_n}{h_n} & \frac{P_n}{h_n} & -\frac{P_n}{h_n} & y_n & \cdot & \end{bmatrix} \begin{bmatrix} y_1 \\ y_2 \\ \vdots \\ y_i \\ \vdots \\ y_n \end{bmatrix} \quad (2.6)$$

in which the square symmetric matrix on the right hand side is referred to as the geometric stiffness matrix of the structure.

The stiffness of the rubber bearings is also reduced by the axial force. The

effect of the axial force on the horizontal stiffness of elastomeric bearings has been studied recently by Chan and Kelly [Ref. 1]. The theoretical results of Chan and Kelly [1] correlated well with experimental data, and it was used herein to investigate the P-delta effect on the dynamic response of base-isolated building structures.

Following Chan and Kelly [1], the horizontal stiffness of a rubber bearing was derived as a series solution, and the first term of the series solution was shown to be a good approximation as follows

$$K_H \approx \frac{GA_s}{L} \left\{ 1 + \frac{\frac{8}{2}}{\pi^2 EI} \frac{\left( 1 + \frac{P}{GA_s} \right)^2}{\frac{GA_s L^2}{GA_s} - \frac{P}{GA_s} \left( 1 + \frac{P}{GA_s} \right)} \right\}^{-1} \quad (2.7)$$

in which  $P$  = compressive force,  $G$  = shear modulus,  $A_s$  = cross-sectional area,  $EI$  = flexural stiffness, and  $L$  = length of the bearing.

When the axial compressive force  $P$  is neglected, the horizontal stiffness, denoted by  $K_b$ , of the bearing is obtained from Eq. (2.7) by setting  $P = 0$  as follows

$$K_b = \left[ \frac{L}{GA_s} + \frac{L^3}{12EI} \right]^{-1} \quad (2.8)$$

Eq. (2.8) gives the horizontal stiffness of a rubber bearing without considering the P-delta effect.

Thus, the reduction of the horizontal stiffness,  $\Delta K$ , for one elastomeric

bearing due to the P-delta effect is given by

$$\Delta K = K_b - K_H \quad (2.9)$$

where  $K_H$  is given by Eq. (2.7).

Finally, the geometric stiffness matrix of the entire structural system, consisting of  $q$  elastomeric bearings and an active mass damper, is obtained by combining Eqs. (2.6) and (2.7) as follows

$$K_G = \begin{bmatrix} 0 & 0 & 0 & 0 \\ 0 & q\Delta K + \frac{P_1}{h_1} & -\frac{P_1}{h_1} & 0 \\ 0 & -\frac{P_1}{h_1} & \frac{P_1}{h_1} + \frac{P_2}{h_2} & -\frac{P_2}{h_2} \\ -\frac{P_i}{h_i} & \frac{P_i}{h_i} + \frac{P_{i+1}}{h_{i+1}} & -\frac{P_{i+1}}{h_{i+1}} & \\ & & -\frac{P_n}{h_n} & \frac{P_n}{h_n} \end{bmatrix} \quad (2.10)$$

The second order matrix equation of motion, Eq. (2.1), can be converted into a first order matrix equation of motion with a dimension of  $2(n+2)$  as follows

$$\dot{\underline{Z}}(t) = \underline{A} \underline{Z}(t) + \underline{B} \underline{U}(t) + \underline{W}_1 \ddot{\underline{X}}_0(t) \quad (2.11)$$

in which  $\underline{Z}(t)$  is a  $(2n+4)$  state vector with the initial condition  $\underline{Z}(0) = 0$ ,

$$\underline{Z}(t) = \begin{bmatrix} \dot{Y}(t) \\ \ddot{Y}(t) \end{bmatrix} \quad (2.12)$$

In Eq. (2.11),  $\underline{A}$  is a  $(2n+4) \times (2n+4)$  system matrix [e.g., 12,13].

For classical linear quadratic optimal control,  $\underline{U}(t)$  is obtained by minimizing the performance index

$$J = \int_0^{t_f} \left[ \underline{Z}'(t) \underline{Q} \underline{Z}(t) + \underline{U}'(t) \underline{R} \underline{U}(t) \right] dt \quad (2.13)$$

in which  $t_f$  = a duration defined to be longer than that of the earthquake,  $\underline{Q} = (2n+4) \times (2n+4)$  positive semi-definite weighting matrix and  $\underline{R} = a (r \times r)$  positive definite weighting matrix [e.g., 12,13].

A minimization of the performance index  $J$ , given by Eq. (2.13), subjected to the constraint of the equations of motion, Eq. (2.11), yields

$$\underline{U}(t) = - (1/2) \underline{R}^{-1} \underline{B}' \underline{P} \underline{Z}(t) \quad (2.14)$$

in which  $\underline{P}$  is a  $(2n+4) \times (2n+4)$  Riccati matrix. Note that Eq. (2.14) is obtained only when the external loading, i.e., the earthquake ground acceleration  $\ddot{X}_0(t)$ , is neglected (or disregarded) [12,13]. Likewise, the solution for the Riccati matrix  $\underline{P}$  is rather cumbersome for a tall building with a large number of degrees of freedom.

Recently, the so-called instantaneous optimal control theory has been proposed by Yang et al. [12,13], where the time dependent quadratic function

$J(t)$  is used as the performance index

$$J(t) = \underline{Z}'(t) \underline{Q} \underline{Z}(t) + \underline{U}'(t) \underline{R} \underline{U}(t) \quad (2.15)$$

Minimizing  $J(t)$  with the constraint of the equations of motion, Eq. (2.11), one obtains the closed-loop instantaneous optimal control law as follows [12,13]

$$\underline{U}(t) = -\frac{\Delta t}{2} \underline{R}^{-1} \underline{B}' \underline{Q} \underline{Z}(t) \quad (2.16)$$

in which  $\Delta t$  is a small time step for the numerical solution of the equations of motion. The implication of minimizing Eq. (2.15) is that the performance index  $J(t)$  is minimized in every small time interval  $(t, t+\Delta t)$  for all  $0 \leq t \leq t_f$ .

It is mentioned that the linear quadratic optimal control law, Eq. (2.14), is limited to linear structures only. However, the instantaneous optimal control law, Eq. (2.16), is applicable to both linear and nonlinear structures [14,15]. Furthermore, there are indications [12] that the performance of the instantaneous optimal control law is better than that of the linear quadratic optimal control law, Eq. (2.14), if the weighting matrix  $\underline{Q}$  is chosen appropriately. Because of the fact that the numerical computation for the Riccati matrix  $\underline{P}$  is quite tedious for tall buildings, the instantaneous optimal control law, Eq. (2.16), is used in this report. The response state vector  $\underline{Z}(t)$  can be solved numerically by substituting Eq. (2.16) into Eq. (2.11).



A sample function of a nonstationary earthquake model is simulated as shown Fig. 3-1, where the maximum ground acceleration  $\ddot{x}_{0\max}$  is 0.3g. Such an earthquake ground acceleration,  $\ddot{x}_0(t)$ , will be used as the input in Eq. (2.11), and the equations of motion will be solved numerically in the time domain to obtain the response quantities of the entire structural system.

### 3.1. Example 1: A Twenty-Story Building

A twenty-story building ( $n=20$ ) in which every story unit is identically constructed is considered in this investigation. The structural properties of each story unit are as follows:  $m_i = m = \text{mass of each floor} = 300 \text{ tons}$ ;  $k_i = k = \text{elastic stiffness of each story unit} = 10^6 \text{ kN/m}$ ;  $c_i = c = \text{internal damping coefficient of each story unit} = 2,261 \text{ kN sec/m}$ . The height of each story is 3 meters. The computed natural frequencies are 0.704, 2.107, 3.498, 4.867, 6.206, 7.507, ..., 17.75, 18.01 and 18.17 Hz. The damping ratio corresponding to the first vibrational mode is 0.5%, and  $\Delta t = 0.015$  second is used.

With the tall building described above and the earthquake ground acceleration shown in Fig. 3-1, time histories of all the response quantities have been computed. The results are almost identical whether or not the P-delta effect is taken into account. Within 30 seconds of the earthquake episode,  $y_i$  and the maximum relative displacement,  $x_i$ , of each story unit (interstory deformation) are shown in Table 3-I(a), where  $x_i = y_i - y_{i-1}$ . Further, the

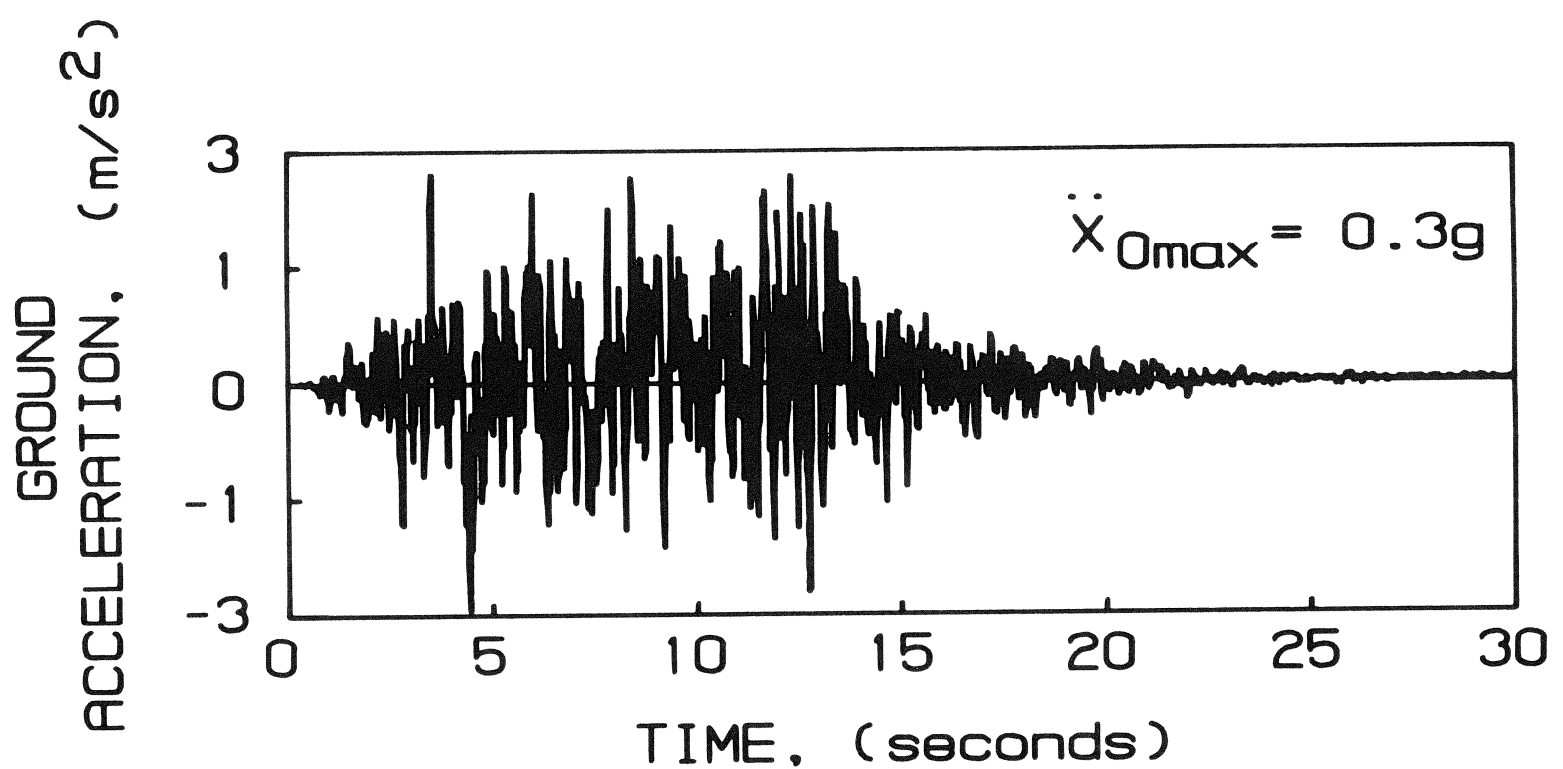


Figure 3-1: A Simulated Earthquake Ground Acceleration.

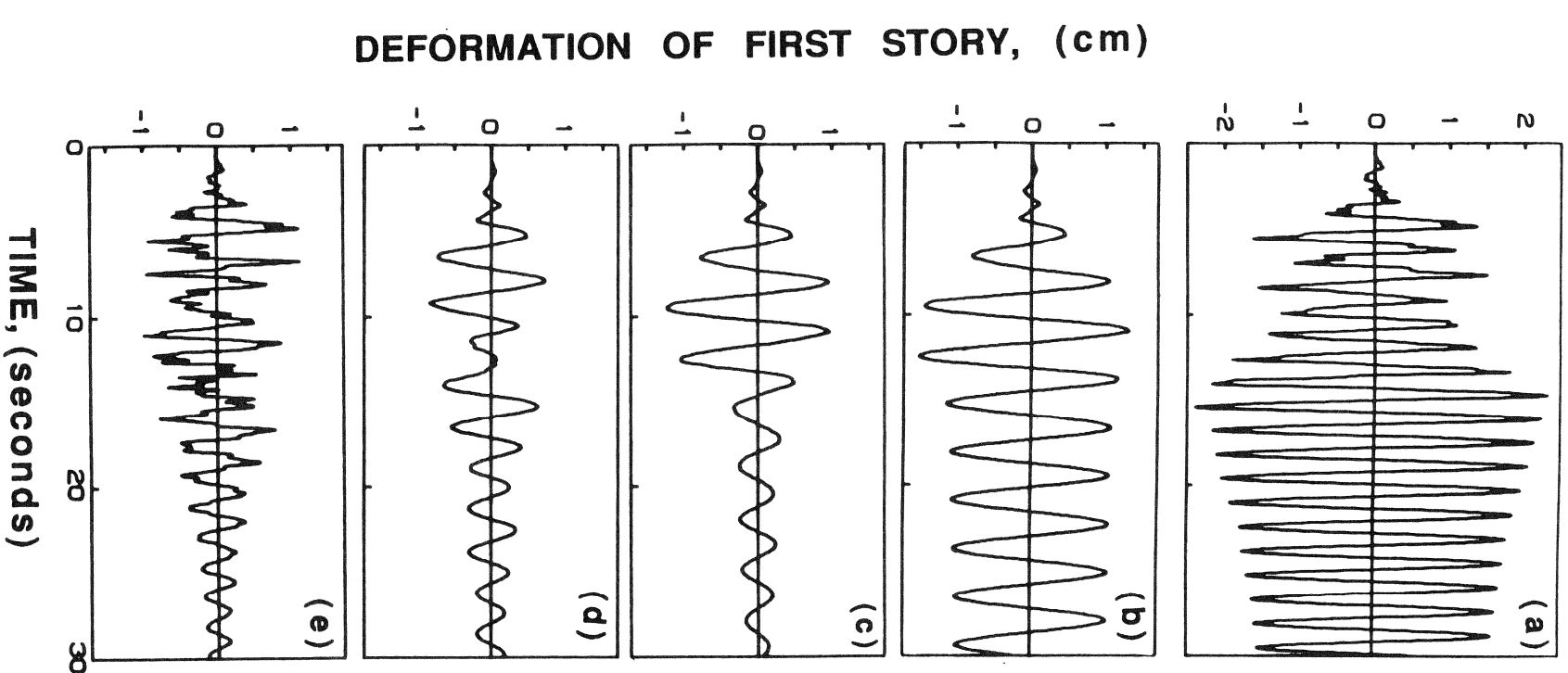


Figure 3-2:  
Deformation of First Story Unit: (a) Building Without Control; (b) With Base Isolation System; (c) With Passive Hybrid Control System ( $m_d=1008 m_1$ ); (d) With Active Hybrid Control System (Control Force = 1031 kN); (e) With Active Control System (Control Force = 1102 kN).

TABLE 3-I: MAXIMUM STRUCTURAL RESPONSE:  
PASSIVE HYBRID CONTROL SYSTEM

(a) WITHOUT P-DELTA EFFECT							
S T O R Y U N I T	WITHOUT ISOLATION		WITH PASSIVE HYBRID CONTROL SYSTEM				
	$m_d = 50\% m_i$	$m_d = 100\% m_i$	$m_d = 200\% m_i$	$m_d = 400\% m_i$	$\bar{y}_d = 1.44 \text{ m}$	$\bar{y}_d = 1.31 \text{ m}$	$\bar{y}_d = 1.08 \text{ m}$
$y_i$ (cm)		$x_i$ (cm)	$x_i$ (cm)	$x_i$ (cm)	$x_i$ (cm)	$x_i$ (cm)	$x_i$ (cm)
B	-	-	40.70	35.67	34.13	31.43	27.48
1	2.39	2.39	1.51	1.33	1.23	1.05	0.76
2	4.78	2.38	1.42	1.28	1.19	1.01	0.72
3	7.13	2.36	1.36	1.23	1.14	0.97	0.69
18	29.94	0.75	0.29	0.28	0.26	0.22	0.17
19	30.30	0.53	0.20	0.19	0.17	0.15	0.11
20	30.48	0.27	0.10	0.09	0.09	0.08	0.06
20*	9.17	3.35	3.13	2.92	2.54	1.89	

(b) WITH P-DELTA EFFECT							
S T O R Y U N I T	WITHOUT ISOLATION		WITH PASSIVE HYBRID CONTROL SYSTEM				
	$m_d = 50\% m_i$	$m_d = 100\% m_i$	$m_d = 200\% m_i$	$m_d = 400\% m_i$	$\bar{y}_d = 1.71 \text{ m}$	$\bar{y}_d = 1.52 \text{ m}$	$\bar{y}_d = 1.20 \text{ m}$
$y_i$ (cm)		$x_i$ (cm)	$x_i$ (cm)	$x_i$ (cm)	$x_i$ (cm)	$x_i$ (cm)	$x_i$ (cm)
B	-	-	52.54	43.60	40.62	35.24	26.77
1	2.39	2.39	1.53	1.25	1.12	0.94	0.65
2	4.78	2.38	1.47	1.20	1.07	0.89	0.61
3	7.13	2.36	1.41	1.15	1.01	0.85	0.58
18	29.94	0.75	0.26	0.22	0.18	0.15	0.12
19	30.30	0.53	0.18	0.15	0.12	0.10	0.08
20	30.48	0.27	0.08	0.07	0.06	0.05	0.04
20*	9.17	2.93	2.44	2.02	1.74	1.38	

maximum acceleration of the top floor in  $\text{m/sec}^2$  is presented in the last row of Table 3-I(a), denoted by  $20^*$ . Under such a strong earthquake,  $\ddot{x}_{0\max} = 0.3g$ , the deformation of the unprotected building is excessive. The time history of the first floor deformation,  $x_1(t)$ , is shown in Fig. 3-2(a).

To reduce the structural response, a rubber-bearing isolation system is implemented, Fig. 2-1(b). The mass of the base isolation system is  $m_b = 400$  tons. The lateral stiffness and viscous damping coefficient are assumed to be linear with  $k_b = 40 \times 10^3 \text{ kN/m}$  and  $c_b = 90.44 \text{ kN.sec/m}$ , respectively. With such a base isolation system, the 21 natural frequencies of the entire building system, without considering the P-delta effect, are 0.35, 1.46, 2.75, 4.06, 5.36, ..., 17.76, 18.0 and 18.17 Hz. The damping ratio for the first vibrational mode of the entire structural system is 0.25%. It is observed that the fundamental frequency is reduced by the implementation of a base isolation system. Time histories of all the response quantities were computed. The time history,  $x_1(t)$ , of the first story deformation is depicted in Fig. 3-2(b), and that of the base isolation system,  $x_b(t)$ , is presented in Fig. 3-3(a). The maximum interstory deformation,  $x_i$ , and the maximum top floor acceleration ( $\text{m/sec}^2$ ) in 30 seconds of the earthquake episode are shown in Table 3-I(a). As observed from Table 3-I(a) and Fig. 3-2, the interstory deformations of the building and the top floor acceleration are drastically reduced. The advantage of using a base isolation system to protect the building is clearly demonstrated. However, the deformation of the base isolation system shown in row B of Table 3-I(a) is excessive.

To examine the P-delta effect, suppose that the base isolation system

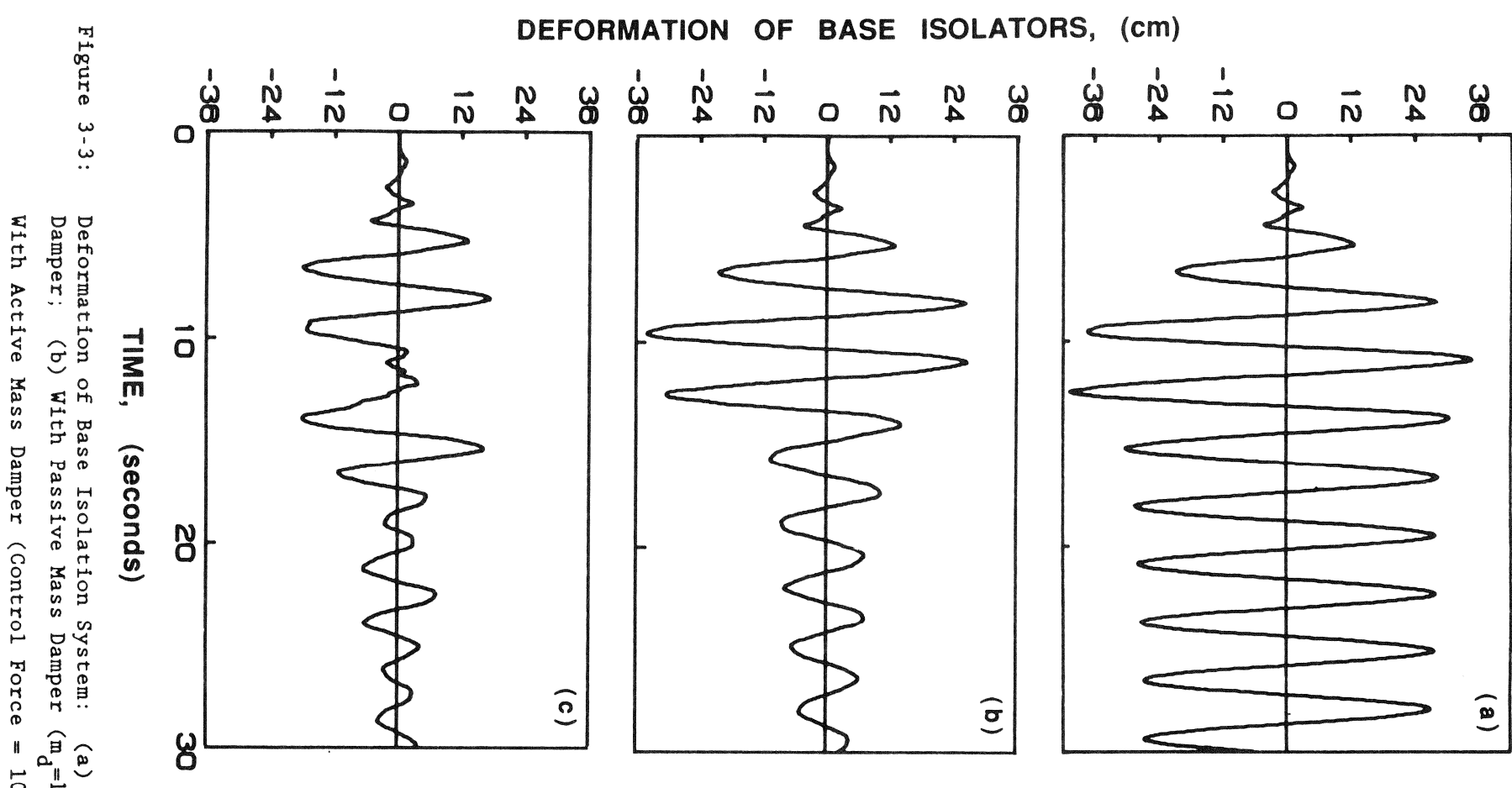


Figure 3-3: Deformation of Base Isolation System: (a) Without Mass Damper; (b) With Passive Mass Damper ( $m_d = 100\% m_1$ ); (c) With Active Mass Damper (Control Force = 1031 kN).

consists of 36 elastomeric bearings each with the following properties:  $L = 0.75$  m,  $G_A_s = 1130 \cdot 12$  kN and  $EI = 148.7$  kNm<sup>2</sup>. The horizontal stiffness of each bearing,  $K_H$ , is computed from Eq. (2.7) as 831.6 kN/m. Hence, the P-delta effect results in a reduction of 25.1% for the horizontal stiffness of the base isolation system. With consideration of the geometric stiffness matrix  $K_G$ , the natural frequencies of the entire building system become 0.31, 1.43, 2.73, 4.03, ..., 17.92 and 18.08 Hz. The damping ratio for the first vibrational mode is 0.29%. It is observed that the P-delta effect reduces the natural frequencies slightly and increases the damping ratio as expected. The maximum response quantities within 30 seconds of the earthquake episode taking into account the P-delta effect are shown in Table 3-I(b).

To protect the safety and integrity of the base isolation system, a passive mass damper is connected to it as shown in Fig. 2-1(a), referred to as the passive hybrid control system. The properties of the mass damper are as follows. The mass of the mass damper  $m_d$  is expressed in term of the  $\gamma$  percentage of the floor mass  $m_i$ , i.e.,  $m_d = \gamma m_i$ , and it will be varied to examine the effect of the mass ratio  $\gamma$ . The natural frequency of the mass damper is the same as the first natural frequency of the base isolated building, i.e., 0.35 Hz without the P-delta effect and 0.31 Hz with the P-delta effect. The damping ratio of the mass damper is 10%.

With such a passive hybrid control system, the maximum deformation of each story unit,  $x_i$ , within 30 seconds of the earthquake episode are presented in Table 3-I for different mass ratio,  $\gamma$ , of the mass damper. Also shown in row B of the table is the maximum deformation of the base isolation system. The maximum deformations for the base isolation system and the first story unit

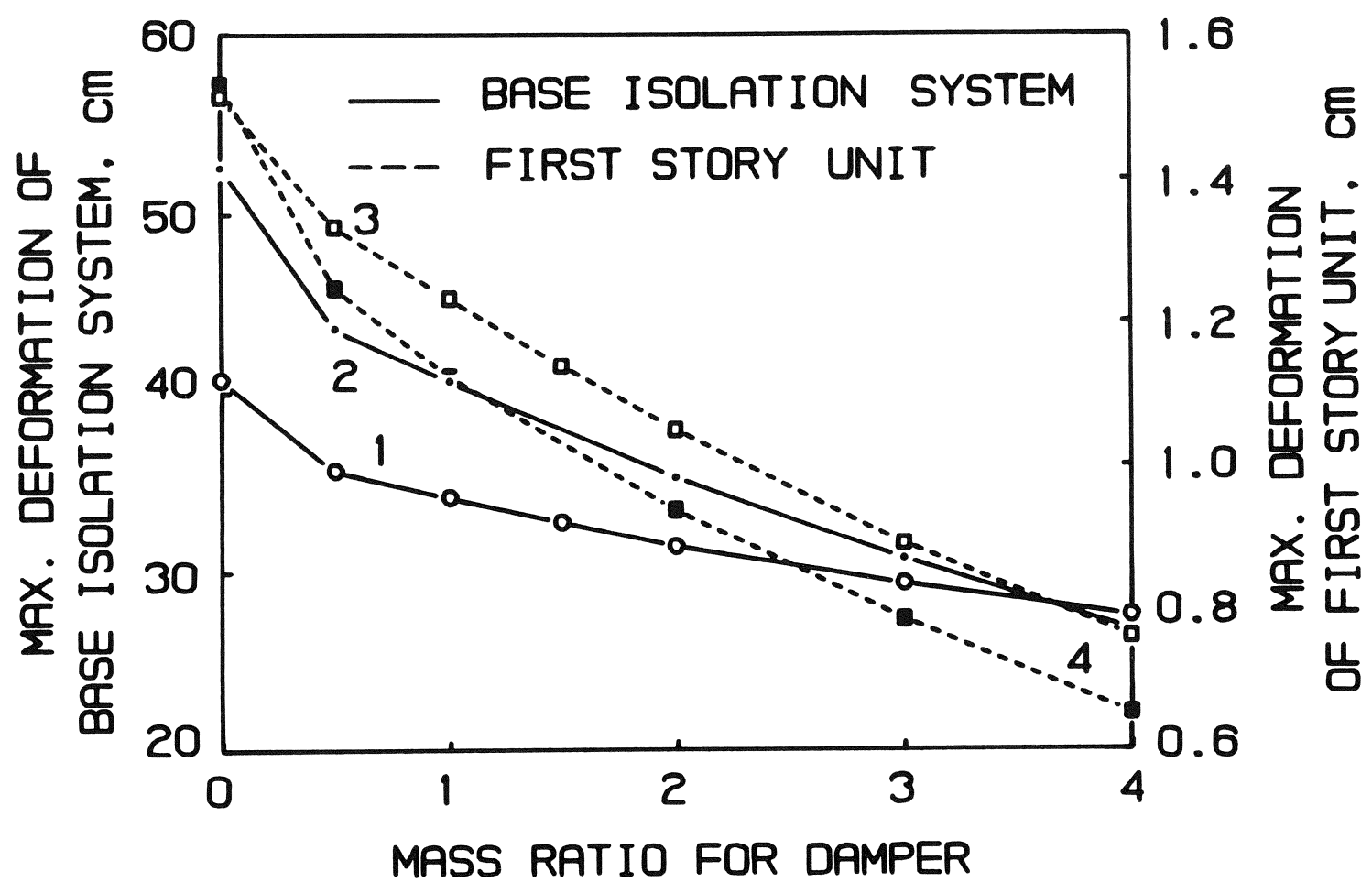


Figure 3-4: Maximum Deformation of First Story Unit and Base Isolation System as Function of Mass Ratio of Passive Damper: (1) Base Isolation System Without P-Delta Effect; (2) Base Isolation System With P-Delta Effect; (3) First Story Unit Without P-Delta Effect; (4) First Story Unit With P-Delta Effect.

are plotted in Fig. 3-4 as a function of the mass ratio  $\gamma = m_d/m_i$ . Note that the first story unit undergoes the largest deformation because of a constant stiffness for all story unit. The maximum relative displacement of the mass damper, denoted by  $\bar{y}_d$ , and the maximum top floor acceleration in  $m/sec^2$  are also shown in Table 3-I. Time histories of the deformations of both the first story unit and the base isolation system are shown in Figs. 3-2(c) and 3-3(b), respectively, for  $\gamma = 1$  and without the P-delta effect. It is observed from Table 3-I that the passive mass damper is capable of reducing not only the deformation of the base isolation system but also the response of the building; the bigger the passive mass damper, the better the performance of the passive hybrid control system.

A comparison between Table 3-I(a) and 3-I(b) indicates that the P-delta effect increases the deformation of the base isolation system. However, the P-delta effect reduces slightly the response of the building structure, because it further removes the natural frequencies of the building structure away from those of the earthquake.

Based on the results above, the passive mass damper appears to be quite effective in protecting the base isolation system. The significant advantage of such a passive hybrid control system is that the passive mass damper is easy to design, install and maintain, especially the mass damper is on the ground level. Thus, the proposed passive hybrid control system is simple for practical implementations.

When a significant reduction for the deformation of the base isolation system is required, the weight of the mass damper (or mass ratio  $\gamma$ ) is large. The

weight of the mass damper can be reduced if an active mass damper shown in Fig. 2-1(b) is used. Let us consider an active mass damper attached to the base isolation system as shown in Fig. 2-1(b). With the application of the active mass damper and the instantaneous optimal control law, Eq. (2.16), the structural response depends on the weighting matrices  $\underline{R}$  and  $\underline{Q}$ . In the present case, the weighting matrix  $\underline{R}$  consists of only one element denoted by  $R$ , whereas the dimension of the  $\underline{Q}$  matrix is  $(44 \times 44)$ .  $R$  is chosen to be  $10^{-3}$  for simplicity. The  $\underline{Q}$  matrix is partitioned as follows [12,13],

$$\underline{Q} = \alpha \begin{bmatrix} 0 & 0 \\ \underline{Q}_{21} & \underline{Q}_{22} \end{bmatrix} \quad (3.1.)$$

in which  $\underline{Q}_{21}$  and  $\underline{Q}_{22}$  are  $(22 \times 22)$  matrices.

For convenience of instrumentation, displacement and velocity sensors are installed on the mass damper and the base isolation system only, i.e., no sensor is installed on the building. In this case, all the elements of  $\underline{Q}_{21}$  and  $\underline{Q}_{22}$  are zero except elements  $\underline{Q}_{21}(1,1)$ ,  $\underline{Q}_{21}(1,2)$ ,  $\underline{Q}_{22}(1,1)$ , and  $\underline{Q}_{22}(1,2)$ , where  $\underline{Q}_{21}(i,j)$  and  $\underline{Q}_{22}(i,j)$  are the  $i-j$  elements of  $\underline{Q}_{21}$  and  $\underline{Q}_{22}$ , respectively. For illustrative purpose, we choose  $\underline{Q}_{21}(1,1) = 0.4$ ,  $\underline{Q}_{21}(1,2) = -900$ ,  $\underline{Q}_{22}(1,1) = 2$  and  $\underline{Q}_{22}(1,2) = 250$ . Furthermore, a mass ratio of 100% for the mass damper is used, i.e.,  $\gamma = 1$ .

The response quantities of the building structures and the base isolation system as well as the required active control force depend on the parameter  $\alpha$ . As the  $\alpha$  value increases, the response quantities reduce, whereas the required active control force increases. Within 30 seconds of the earthquake episode, the maximum deformation of the base isolation system, the maximum

TABLE 3-II: MAXIMUM STRUCTURAL RESPONSE:  
ACTIVE HYBRID CONTROL SYSTEM

(a) WITHOUT P-DELTA EFFECT					
S T O R Y U N I T	WITHOUT CONTROL SYSTEM	WITH BASE CONTROL SYSTEM	WITH ACTIVE HYBRID CONTROL SYSTEM		
			WITH PASSIVE HYBRID SYSTEM $m_d = 100\% m_i$	WITH ACTIVE HYBRID SYSTEM $m_d = 100\% m_i$	WITH ACTIVE HYBRID SYSTEM $m_d = 100\% m_i$
B	-	$\alpha/R=30 \times 10^3$	$\alpha/R=14 \times 10^4$	$\alpha/R=22 \times 10^4$	
1	2.39	40.70	34.13	31.43	22.61
2	2.38	1.51	1.23	1.14	0.93
3	2.36	1.42	1.19	1.10	0.90
18	0.75	1.36	1.14	1.06	0.86
19	0.53	0.29	0.26	0.24	0.20
20	0.27	0.20	0.17	0.17	0.14
		0.10	0.09	0.08	0.07
20*	9.17	3.35	2.92	2.77	2.29
					1.99
(b) WITH P-DELTA EFFECT					
S T O R Y U N I T	WITHOUT CONTROL SYSTEM	WITH BASE CONTROL SYSTEM	WITH ACTIVE HYBRID CONTROL SYSTEM		
			WITH PASSIVE HYBRID SYSTEM $m_d = 100\% m_i$	WITH ACTIVE HYBRID SYSTEM $m_d = 100\% m_i$	WITH ACTIVE HYBRID SYSTEM $m_d = 100\% m_i$
B	-	$\alpha/R=30 \times 10^3$	$\alpha/R=14 \times 10^4$	$\alpha/R=24 \times 10^4$	
1	2.39	$\bar{y}_d = 1.86 \text{ m}$	$\bar{y}_d = 2.77 \text{ m}$	$\bar{y}_d = 3.30 \text{ m}$	
2	2.38	$m_d = 100\% m_i$	$U=274.77 \text{ kN}$	$U=833.25 \text{ kN}$	$U=1223.8 \text{ kN}$
3	2.36	$\bar{y}_d = 1.52 \text{ m}$	$\dot{U}=1044.1 \text{kN}/\text{sec.}$	$\dot{U}=4473.4 \text{kN}/\text{sec.}$	$\dot{U}=7211.5 \text{kN}/\text{sec.}$
18	0.75				
19	0.53				
20	0.27				
20*	9.17	2.93	2.02	1.95	1.91
					1.87

interstory deformation,  $x_i$ , the required maximum control force,  $U$ , the maximum control force rate,  $\dot{U} = dU/dt$ , and the maximum top floor acceleration in  $m/sec^2$  are summarized in Table 3-II for different values of  $\alpha/R$ . Table 3-II(a) shows the results without accounting for the P-delta effect, whereas Table 3-II(b) presents the corresponding results with the P-delta effect. Some results are plotted in Figs. 3-5 and 3-6. Time histories of the deformations of the first story unit and the base isolation system are shown in Figs. 3-2(d) and 3-3(c), respectively, for  $\alpha/R = 22 \times 10^5$  for the case in which the P-delta effect is neglected. It is observed from Table 3-II and Figs. 3-5 and 3-6 that the response quantities reduce as the active control force increases.

Within 30 seconds of the earthquake episode, the maximum displacement of the building system is plotted in Fig. 3-7 for comparison. Curve 1 in Fig. 3-7 represents the maximum response of the building without control. Curve 2 denotes the maximum response of the building with a base isolation system, where the maximum deformation of the base isolation system is indicated by the story level 0. The maximum response of the building implemented by the passive hybrid control system is shown by Curve 3, where the mass ratio of the damper is 100%. The corresponding result for the building implemented by the active hybrid control system is depicted by Curve 4, where the mass ratio of the damper is 100% and the maximum control force is 1031 kN. Curves 2-4 represent the results without taking into account the P-delta effect. The corresponding results, when the P-delta effect is accounted for, are presented by Curves 5-7, respectively, where the maximum control force for the active hybrid control system is 1224 kN. Tables 3-I and 3-II as well as

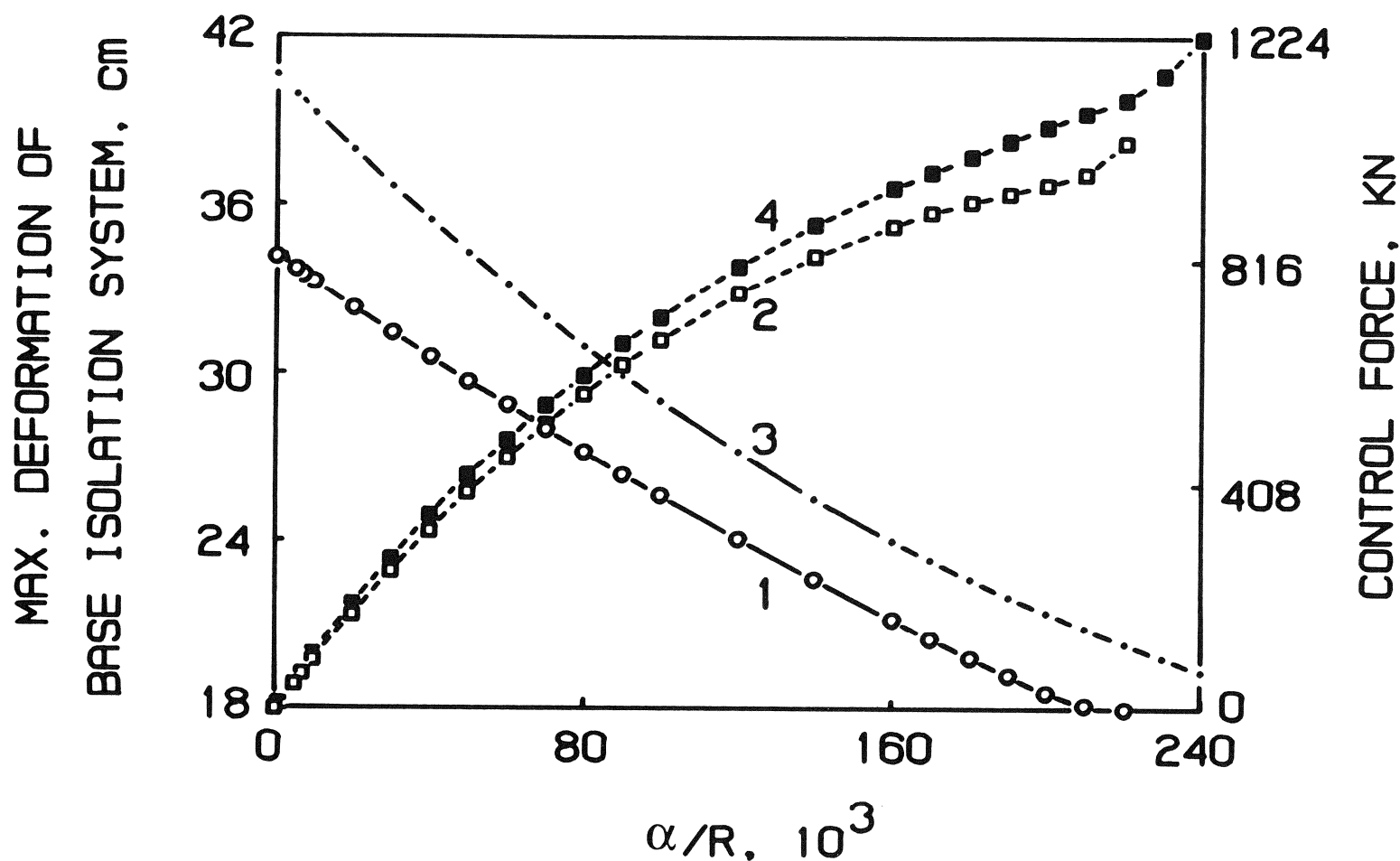


Figure 3-5: Maximum Deformation of Base Isolation System and Maximum Control Force as Function of  $\alpha/R$ : (1) Base Isolation System Without P-Delta Effect; (2) Control Force Without P-Delta Effect; (3) Base Isolation System With P-Delta Effect; (4) Control Force With P-Delta Effect.

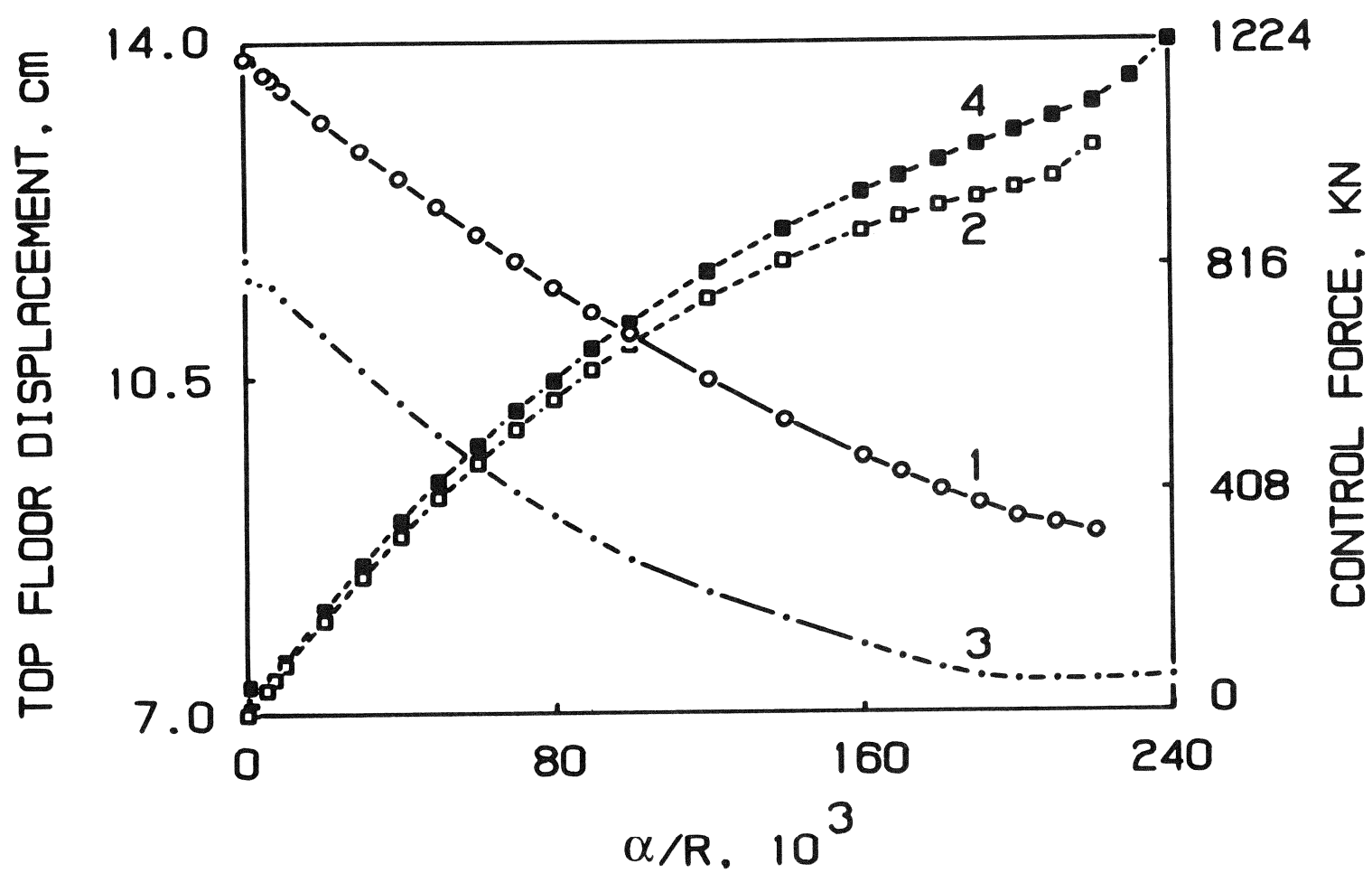


Figure 3-6: Maximum Displacement of The Top Floor Relative to The Base and Maximum Control Force as Function of  $\alpha/R$ : (1) Top Floor Displacement Without P-Delta Effect; (2) Control Force Without P-Delta Effect; (3) Top Floor Displacement with P-Delta Effect; (4) Control Force With P-Delta Effect.

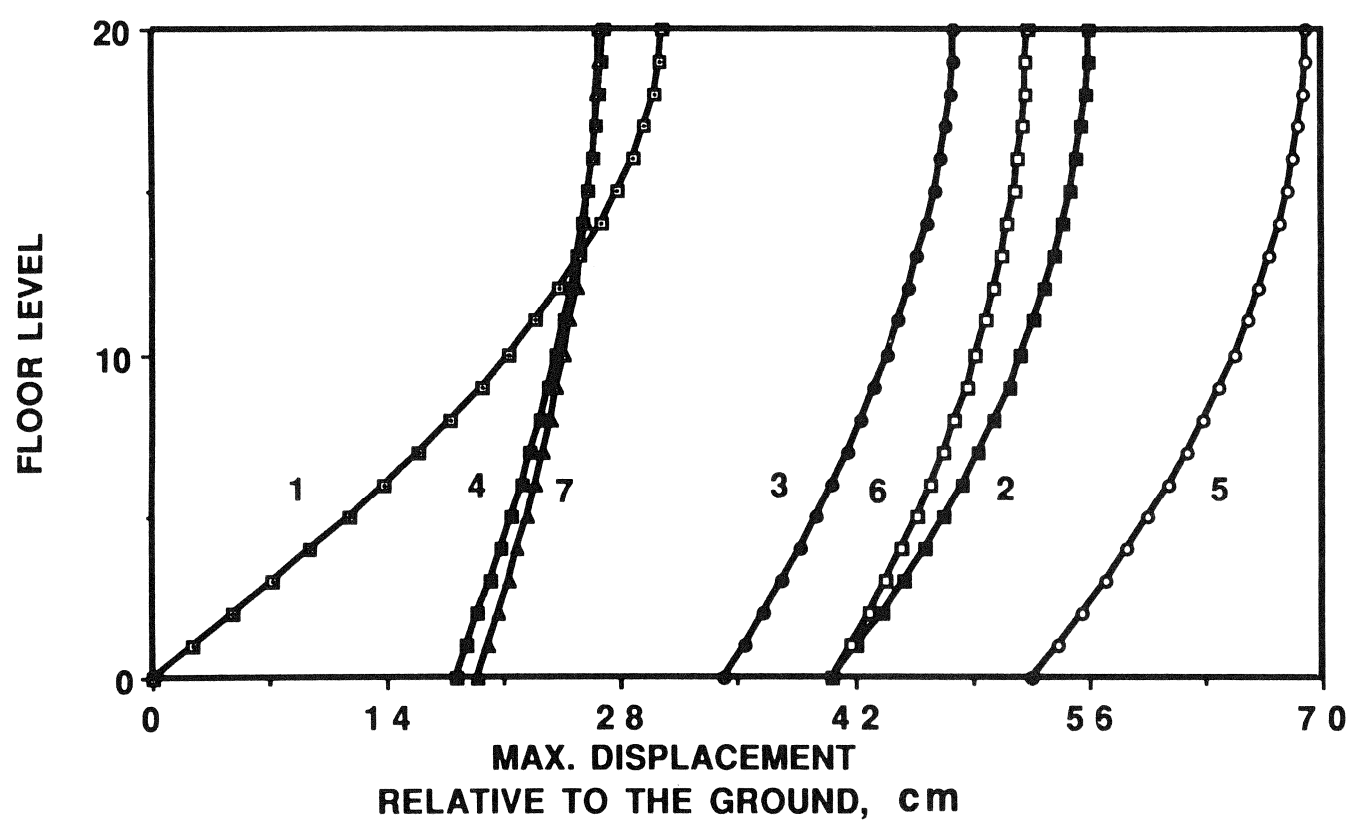


Figure 3-7: Maximum Displacement of The Structural System With Respect to The Ground: (1) Without Control; (2) Base Isolation System Without P-Delta Effect; (3) Passive Hybrid Control System Without P-Delta Effect (Mass Ratio 100%); (4) Active Hybrid Control System Without P-Delta Effect; (5) Base Isolation System With P-Delta Effect; (6) Passive Hybrid Control System With P-Delta Effect; (7) Active Hybrid Control System With P-Delta Effect.

Fig. 3-7 clearly demonstrate the effectiveness of the two hybrid control systems proposed.

Consider the case in which the 20-story building is implemented by an active control system alone; namely, an active mass damper on the top floor as shown in Fig. 1(a). Again, the instantaneous optimal control law, Eq. (2.16), will be used and the (42x42) weighting matrix  $\underline{Q}$  is partitioned as shown in Eq. (3.1). The dimension of  $\underline{Q}_{21}$  and  $\underline{Q}_{22}$  matrices is (2x21). For illustrative purpose, elements of these matrices are chosen as follows. The first row of  $\underline{Q}_{21}$  matrix is (-12, -12, -13.5, -16, -17.5, -19, -20.5, -22, -23.5, -25, -26.5, -28, -29.5, -31, -32.5, -34, -35.5, -37, -38.5, -40, 1) and the second row of  $\underline{Q}_{22}$  is identical to the first row above. The first row of  $\underline{Q}_{21}$  matrix is (-500, -500, -510, -510, -540, -580, -610, -640, -670, -700, -730, -760, -790, -820, -850, -880, -910, -940, -1000, -3900, 800). The second row of  $\underline{Q}_{21}$  matrix is identical to the first row except the last element 800 that is replaced by 100. Since the active mass damper is installed on the top floor, a mass ratio of 10%, i.e.,  $m_d = 10\% m_i$ , is considered. Note that for this active mass damper control system, displacement and velocity sensors are installed on every floor of the building. For the active hybrid control system presented previously, however, displacement and velocity sensors are installed only on the base isolation system and the mass damper, i.e., no sensor is installed on building floors.

Time histories of all the response quantities were computed for different values of  $\alpha/R$ . The deformation of the first story unit,  $x_1(t)$ , is plotted in Fig. 3-2(e) for comparison, in which the maximum active control force is  $U =$

TABLE 3-III: MAXIMUM STRUCTURAL RESPONSE  
ACTIVE MASS DAMPER ALONE

S T O R Y U N I T	WITHOUT CONTROL	WITH PASSIVE MASS DAMPER	WITH ACTIVE MASS DAMPER $m_d = 10\% m_i$	
			$\alpha/R = 300$	$\alpha/R = 3000$
		$m_d = 10\% m_i$	$\bar{x}_d = 1.55 \text{ m}$	$\bar{x}_d = 5.67 \text{ m}$
			$U = 149 \text{ kN}$	$U = 1102 \text{ kN}$
		$\dot{x}_d = 0.94 \text{ m}$	$\dot{U} = 678 \text{ kN/sec.}$	$\dot{U} = 5476 \text{ kN/sec.}$
				$\dot{U} = 7315 \text{ kN/sec.}$
$x_i$		$x_i$	$x_i$	$x_i$
(cm)		(cm)	(cm)	(cm)
1	2.39	1.59	1.52	1.13
2	2.38	1.56	1.49	1.09
3	2.36	1.49	1.42	1.06
18	0.75	0.64	0.6	0.53
19	0.53	0.45	0.42	0.47
20	0.27	0.22	0.21	0.39
20*	9.17	8.28	7.91	5.86
				5.18

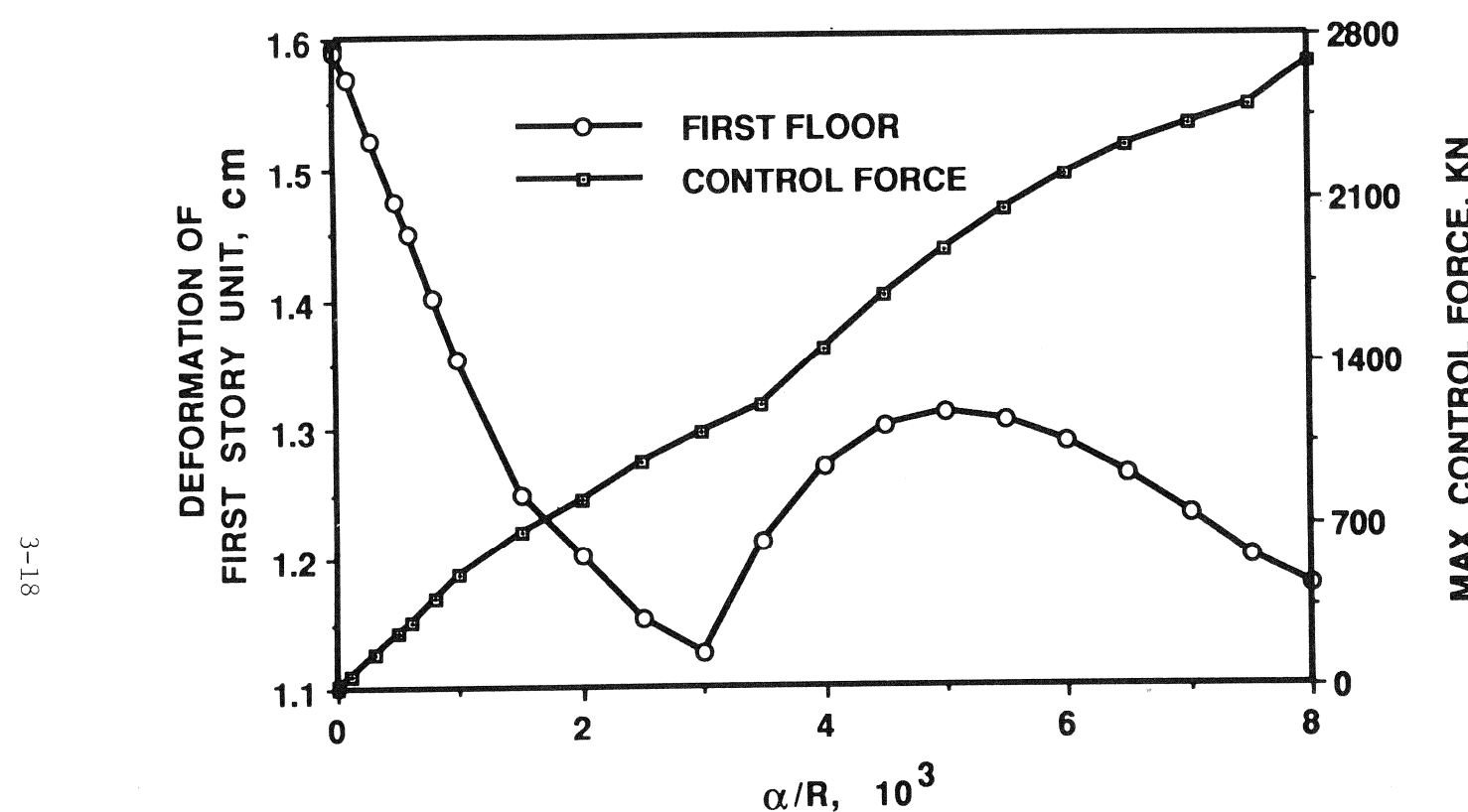


Figure 3-8: Maximum Deformation of First Story Unit and Maximum Control Force as Function of  $\alpha/R$  (Active Mass Damper on Top Floor).

1102 kN and the maximum control force rate is  $\dot{U} = 5476 \text{ kN/sec}$ . Within 30 seconds of the earthquake episode, the following quantities are summarized in Table 3-III: (i) the maximum interstory deformation,  $x_i$ , (ii) the maximum relative displacement of the mass damper with respect to the top floor,  $\bar{x}_d$ , (iii) the maximum active control force  $U$ , and (iv) the maximum time derivative of the control force  $\dot{U}$ , and (v) the maximum top floor acceleration in  $\text{m/sec}^2$ . The maximum deformation of the first story unit versus the maximum required active control force is plotted in Fig. 3-8. In addition, the maximum response quantities using a passive mass damper ( $m_d = 10\% m_i$ ) installed on the top floor are shown in Table 3-III for comparison.

Examination of extensive numerical results indicates that a reduction of 50% for the first story deformation and the maximum top floor acceleration is probably the maximum limit that can be achieved by one active mass damper. On the other hand, a reduction of more than 50% for the first story deformation and the maximum top floor acceleration can easily be accomplished using either one of the hybrid control systems proposed. Thus, for the protection of tall buildings against strong earthquakes, the proposed hybrid control systems may have significant advantages over the application of an active control system alone.

### 3.2. Example 2: A Laboratory Scaled Five-Story Building

Instead of the tall building considered in Example 1, the performance of the two hybrid control systems for low-rise buildings will be investigated and evaluated. A laboratory scaled five-story building [Refs. 21-23] is considered for illustrative purposes. The floor masses are identical with  $m_i$

$(i = 1, 2, \dots, 5) = 5.9$  tons. The stiffness of each story unit is assumed to be linear elastic with  $k_i = 33.732 \times 10^3$ ,  $29.093 \times 10^3$ ,  $28.621 \times 10^3$ ,  $24.954 \times 10^3$ ,  $19.059 \times 10^3$  kN/m for  $i = 1, 2, \dots, 5$ , and the internal damping coefficients for each story unit are  $c_i = 67, 58, 57, 50, 38$  kN.sec/m, respectively. This corresponds to a 2% damping for the first vibrational mode of the building. The computed natural frequencies are 3.20, 8.71, 13.61, 17.59 and 20.91 Hz. The same simulated earthquake record shown in Fig. 3-1 with a maximum ground acceleration of  $\ddot{x}_{0\max} = 0.3g$  is used as the input excitation. Time histories for the displacement of each floor have been computed. Without any control system, the maximum relative displacement of each floor with respect to the ground  $y_i$  ( $i = 1, 2, \dots, 5$ ) and the maximum interstory deformation  $x_i$  ( $i = 1, 2, \dots, 5$ ) within 30 seconds of the earthquake episode are shown in Table 3-IV. The P-delta effect on the dynamic response of the building is negligible. The time history of the deformation of the first story unit is presented in Fig. 3-9(a).

**Structure With Base Isolation System:** The structure is implemented by a base isolation system consisting of 4 rubber bearings. The properties of each bearing are:  $L = \text{length} = 20$  cm,  $G_A_S = 60.86$  kN and  $EI = 11.97$  kN.m<sup>2</sup>. The horizontal stiffness of the entire base isolation system without accounting for the P-delta effect is  $4K_b = 1,200$  kN/m, Eq. (2.8). With the P-delta effect, where the weight of the building is accounted for, the horizontal stiffness of the base isolation system is  $4K_H = 1,035$  kN/m, Eq. (2.7). The mass of the base isolation system is  $m_b = 6.8$  tons and the linear viscous damping of the base isolation system is  $c_b = 2.4$  kN.sec/m. With the base isolation system above and neglecting the P-delta effect, the natural frequencies of the entire building system are 0.89, 5.56, 10.33, 14.73, 18.41

TABLE 3-IV: MAXIMUM STRUCTURAL RESPONSE:  
(FIVE-STORY MODEL)

PASSIVE HYBRID CONTROL SYSTEM

(a) WITHOUT P-DELTA EFFECT					
S T O R Y U N I T	WITHOUT ISOLATION		WITH PASSIVE HYBRID CONTROL SYSTEM		
	$m_d = 0.1 m_i$	$m_d = 0.2 m_i$	$m_d = 0.3 m_i$	$m_d = 0.4 m_i$	
B	$\bar{y}_d = 37.61\text{cm}$	$\bar{y}_d = 27.0\text{cm}$	$\bar{y}_d = 24.22\text{cm}$	$\bar{y}_d = 22.24\text{cm}$	
1	1.29	1.29	0.42	0.28	0.20
2	2.69	1.40	0.4	0.26	0.19
3	3.91	1.22	0.3	0.20	0.17
4	4.94	1.03	0.23	0.15	0.15
5	5.67	0.73	0.15	0.10	0.09

(b) WITH P-DELTA EFFECT					
S T O R Y U N I T	WITHOUT BASE ISOLATION		WITH PASSIVE HYBRID CONTROL SYSTEM		
	$m_d = 0.1 m_i$	$m_d = 0.2 m_i$	$m_d = 0.3 m_i$	$m_d = 0.4 m_i$	
B	$\bar{y}_d = 44.56\text{cm}$	$\bar{y}_d = 34.85\text{cm}$	$\bar{y}_d = 31.12\text{cm}$	$\bar{y}_d = 29.39\text{cm}$	
1	-	-	-	-	-
2	1.29	1.29	0.43	0.25	0.21
3	2.69	1.40	0.41	0.23	0.19
4	3.91	1.22	0.32	0.18	0.15
5	4.94	1.03	0.25	0.14	0.11
	5.67	0.73	0.16	0.09	0.08

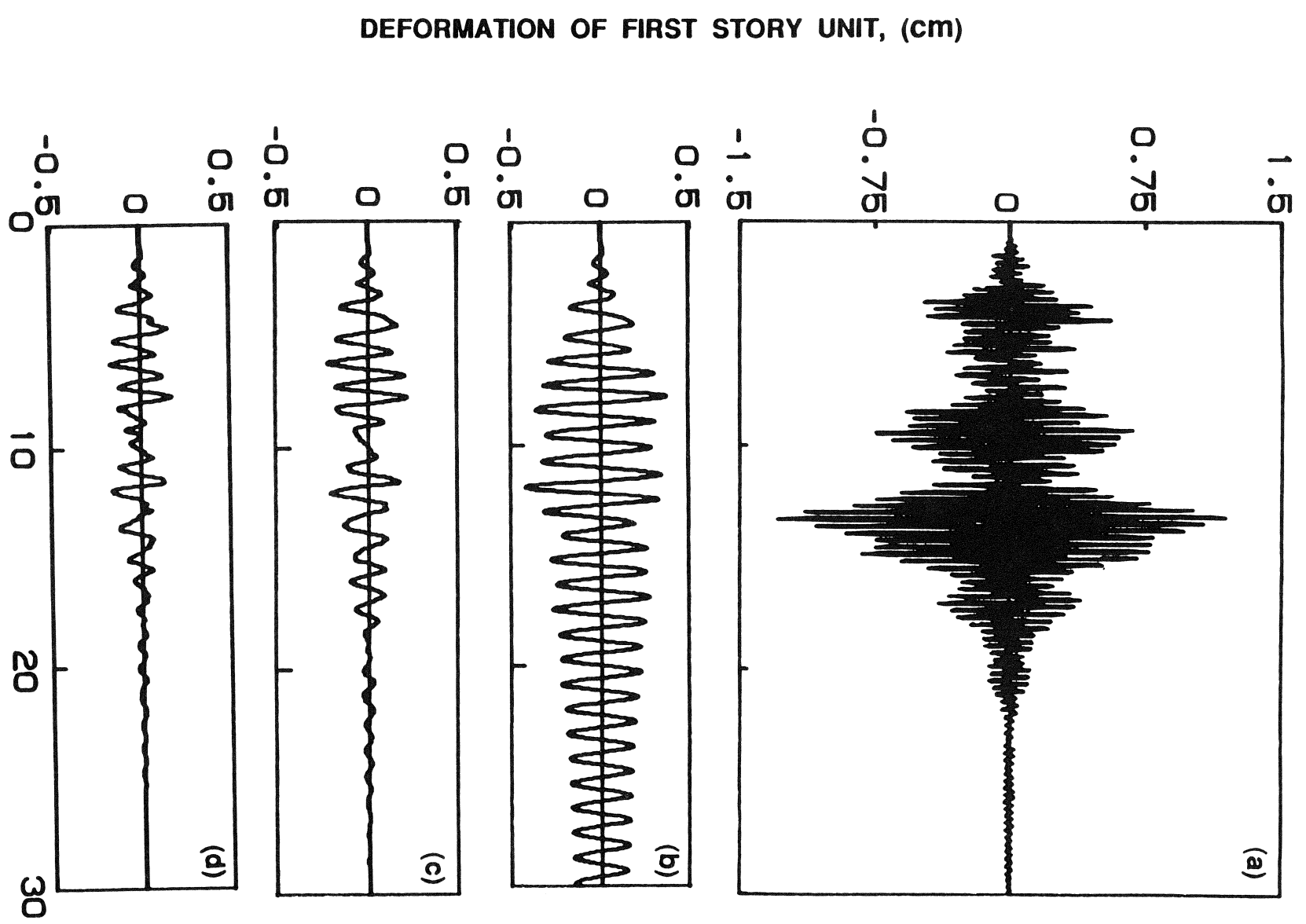


Figure 3-9: Deformation of First Story Unit: (a) Building Without Control; (b) With Base Isolation System; (c) With Passive Hybrid Control System ( $m_d=20\% m_i$ ); (d) With Active Hybrid Control System ( $m_d=10\% m_i$  and  $\alpha/R=30$ ).

and 21.31 Hz. The damping ratio for the first vibrational mode of the entire system is 0.55%. It is observed that the fundamental frequency of the system is reduced by 72%.

Taking into consideration the P-delta effect, the geometric stiffness matrix,  $\underline{K}_G$ , is computed. The natural frequencies of the building system become 0.83, 5.52, 10.30, 14.69, 18.35 and 21.25 Hz. The damping ratio for the first vibrational mode is 0.6%. A comparison with the structure without accounting for the P-delta effect indicates that the natural frequencies are reduced slightly, whereas the damping ratio increases as expected.

The maximum interstory deformations  $x_i$  ( $i = 1, 2, \dots, 5$ ) of the building are shown in Table 3-IV for both cases in which the P-delta effect is and is not accounted for. The deformation of the base isolation system is presented in row B of Table 3-IV. As observed from Table 3-IV, the interstory deformations of the building are drastically reduced and the building moves like a rigid body. The advantage of using a base isolation system to protect the building is clearly demonstrated. However, the deformation of the base isolation system is excessive and it should be protected by other devices. It is further observed from Table 3-IV that the P-delta effect is insignificant for the building response even if the building is base-isolated. However, the P-delta effect results in an increase of about 17% for the response of the base isolation system. Time histories of the deformations of the first story unit and the base isolation system are shown in Fig. 3-9(b) and 3-10(a), respectively, in which the P-delta effect is neglected.

Structure With Passive Hybrid Control System: For the passive hybrid control

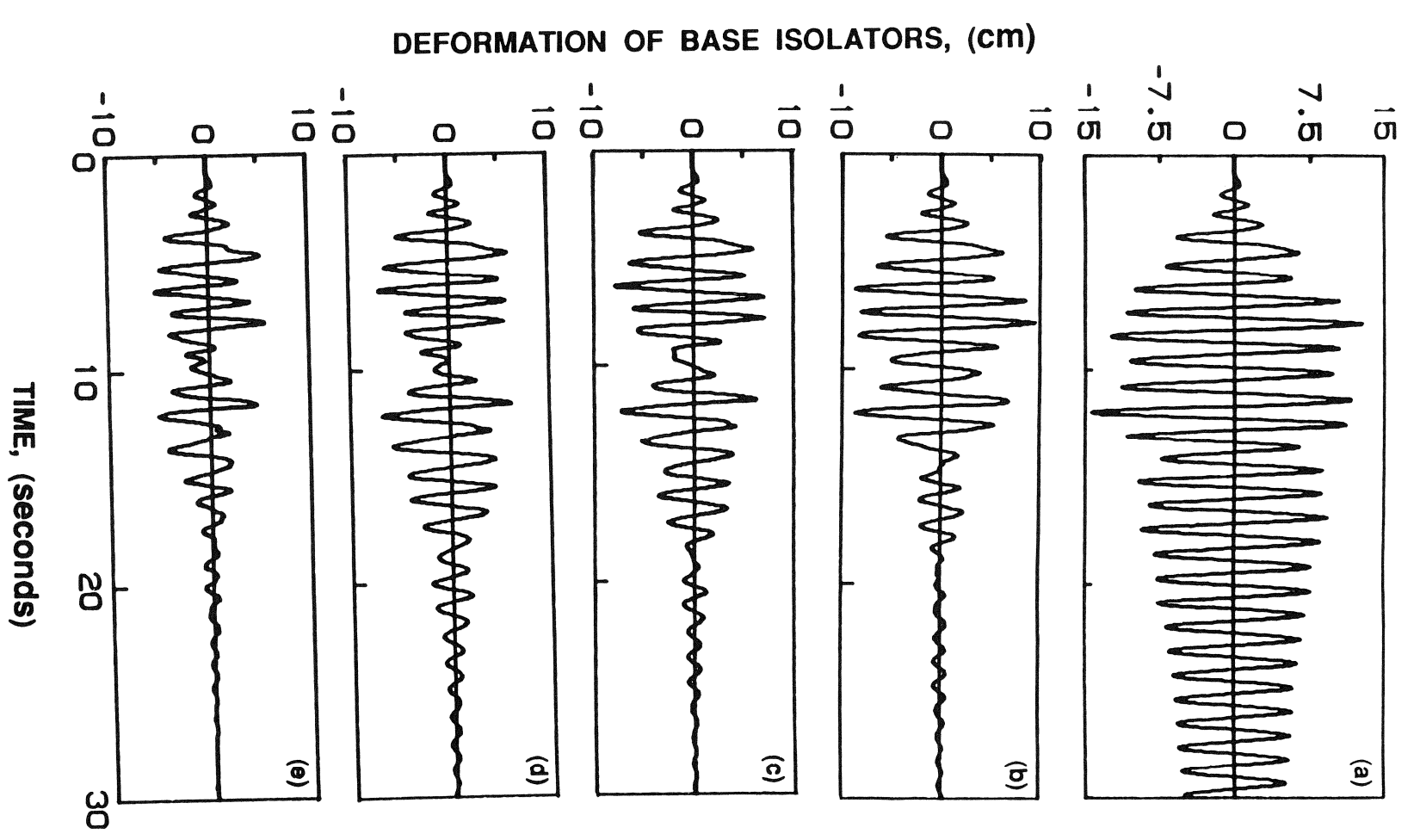


Figure 3-10: Deformation of Base Isolation System: (a) Without Mass Damper; (b) With Passive Mass Damper  $m_d = 10\% m_i$ ; (c)  $m_d = 20\% m_i$ ; (d)  $m_d = 30\% m_i$ ; (e) With Active Mass Damper ( $m_d = 10\% m_i$ ,  $\alpha/R = 30$ ).

system, Fig. 2-1(a), the mass damper for the base isolation system has the following properties: (a) Four different masses for the mass damper are considered. These are 10%, 20%, 30% and 40% of the floor mass, respectively,

(b) The frequency of the mass damper is 98% of the first natural frequency of the building including the base isolation system; namely,  $0.98 \times 0.89 \text{ Hz} = 0.87 \text{ Hz}$  without the P-delta effect and  $0.98 \times 0.83 = 0.813 \text{ Hz}$  with the P-delta effect, and (c) The damping ratio is 10% of the critical damping of the mass damper. With such a passive hybrid control system, the response time histories of the structure have been computed.

Within 30 seconds of the earthquake episode, the maximum interstory deformations  $x_i$  ( $i = 1, 2, \dots, 5$ ) of the building system with different mass dampers are summarized in Table 3-IV for both cases in which the P-delta effect is and is not taken into account. Also shown in Table 3-IV is the maximum relative displacement of the mass damper,  $\bar{y}_d$ , with respect to the ground. Time histories for the deformation of the base isolation system are presented in Figs. 3-10(b) - (d) for different mass dampers and for the case in which the P-delta effect is neglected. Further, the time history of the deformation of the first story unit is presented in Fig. 3-9(c) for  $m_d = 20\% m_i$ .

It is observed from Table 3-IV and Fig. 3-10 that a reduction of 35%, 46%, 51% and 55% for the response of the base isolation system has been achieved using four different mass dampers. It is further observed from Table 3-IV and Fig. 3-9 that the mass damper is capable of reducing the response quantities of the building in addition to protecting the base isolation system. Finally, the maximum deformations of the base isolation system within 30 seconds of the earthquake episode with or without accounting for

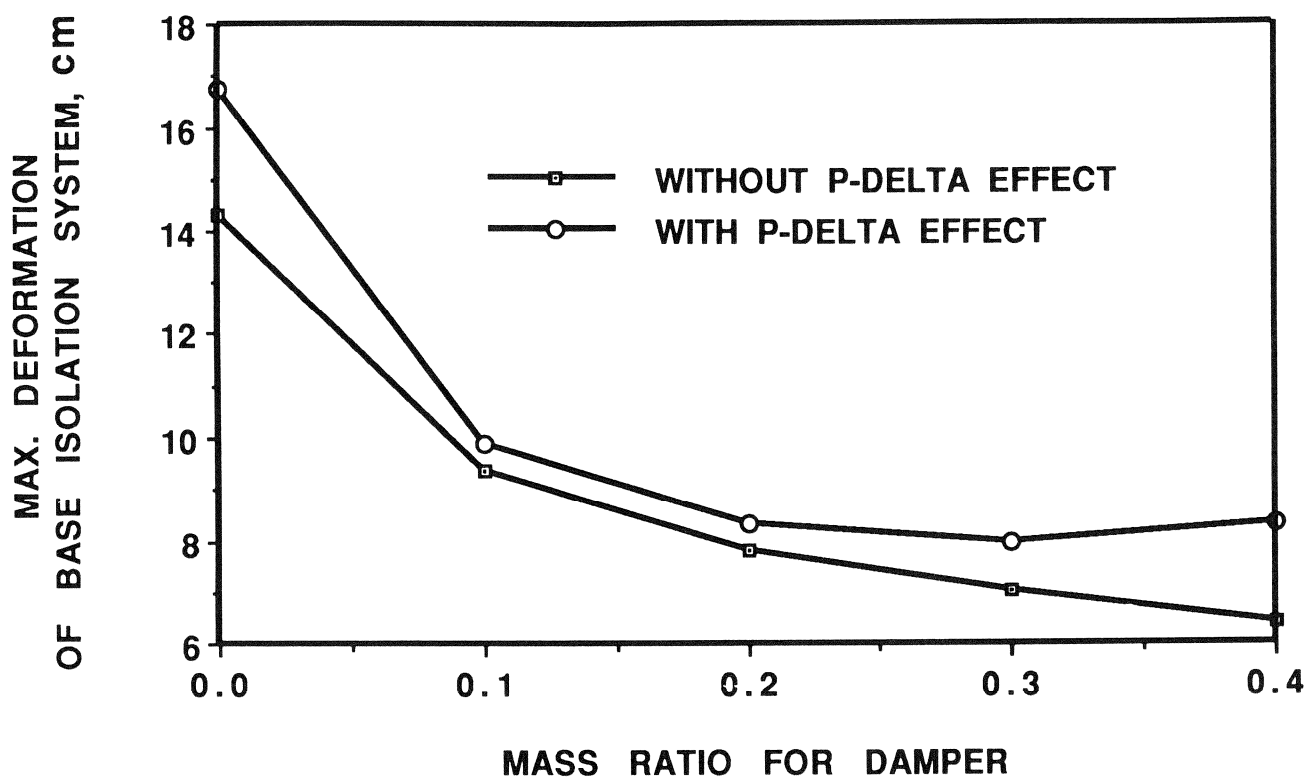


Figure 3-11: Maximum Deformation of Base Isolation System as a Function of mass ratio  $\gamma = m_d/m_i$ .

the P-delta effect are displayed in Fig. 3-11 for different mass dampers. A general trend observed from this figure is that the bigger (or heavier) the mass damper, the more effective the passive hybrid control system.

The observations obtained from Table 3-IV and Figs. 3-9 through 3-11 are summarized as follows: (i) While the base isolation system alone is capable of protecting the building structure, its deformation may be excessive under strong earthquakes; (ii) The deformation of the base isolation system can be reduced by the use of a passive mass damper attached to the base isolation system; (iii) The passive mass damper is capable of reducing not only the response of the base isolation system but also the response of the building; (iv) The bigger (or heavier) the passive mass damper, the better the performance of the mass damper; and (v) the P-delta effect on the building response is minimal and its effect on the response of the base isolation system is to increase the response by 15-20%. These observations are similar to those obtained previously for the twenty-story building.

**Structure With Active Hybrid Control System:** Instead of using a passive mass damper for protecting the base isolation system, an active mass damper is considered herein. With the active mass damper, the structural response depends on the weighting matrices  $\underline{R}$  and  $\underline{Q}$ . For this example, the weighting matrix  $\underline{R}$  consists of only one element denoted by  $R$ , whereas the dimension of the  $\underline{Q}$  matrix is  $(14 \times 14)$ .  $R$  is chosen to be  $10^{-3}$  for simplicity. The  $\underline{Q}$  matrix is partitioned as shown in Eq. (3.1) in which  $Q_{21}$  and  $Q_{22}$  are  $(7 \times 7)$  matrices.

Again, for convenience of instrumentation, displacement and velocity sensors

are installed on the active mass damper and the base isolation system only, i.e., no sensor is installed on the building. In this case, all elements of matrices  $\underline{Q}_{21}$  and  $\underline{Q}_{22}$  are zero except  $Q_{21}(1,1)$ ,  $Q_{21}(1,2)$ ,  $Q_{22}(1,1)$  and  $Q_{22}(1,2)$ , where  $Q_{21}(i,j)$  and  $Q_{22}(i,j)$  are the  $i-j$  elements of  $\underline{Q}_{21}$  and  $\underline{Q}_{22}$ , respectively. For simplicity, the following values are assigned:  $Q_{21}(1,1) = 90$ ,  $Q_{21}(1,2) = -800$ ,  $Q_{22}(1,1) = 10$  and  $Q_{22}(1,2) = 250$ . The mass ratio of the mass damper is 10%, i.e.,  $m_d = 10\% m_1$ .

Time histories of the structural response quantities for different  $\alpha/R$  values have been computed. In particular, the time histories of the deformation of the base isolation system and the first story unit are shown in Fig. 3-10(e) and 3-9(d), respectively, for  $\alpha/R = 30$  without accounting for the P-delta effect. The required active control force is displayed in Fig. 3-12.

Within 30 seconds of the earthquake episode, the maximum deformations  $x_i$  ( $i = B, 1, 2, \dots, 5$ ) of the building system, the maximum active control force  $U$  and force rate  $\dot{U}$ , as well as the maximum relative displacement of the mass damper  $\bar{y}_d$  are summarized in Table 3-V. The maximum deformation of the base isolation system and the required maximum control force are plotted in Fig. 3-13 as a function of  $\alpha/R$ .

The following conclusions are obtained based on the observations of Table 3-V and Figs. 3-9(d), 3-10(e), 3-12 and 3-13; (i) The active hybrid control system proposed herein is very effective in protecting not only the base isolation system but also the building itself, and (ii) a drastic reduction for the response of the base isolation system up to 60% can be achieved by the active mass damper without a large control force.

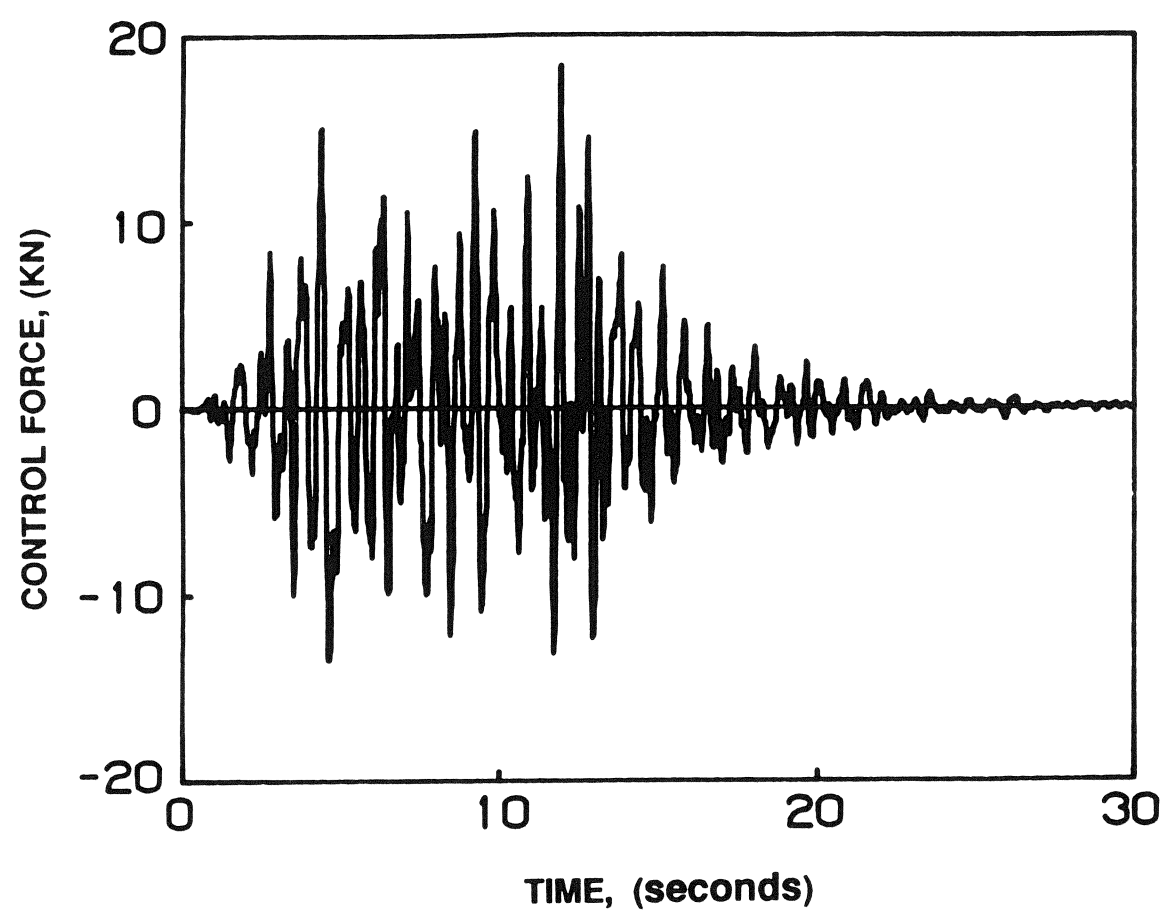


Figure 3-12: Required Active Control Force With  $m_d=10\% m_i$  and  $\alpha/R=30$ .

TABLE 3-V: MAXIMUM STRUCTURAL RESPONSE  
(FIVE-STORY MODEL)  
ACTIVE HYBRID CONTROL SYSTEM

(a) WITHOUT P-DELTA EFFECT					
S T O R Y	WITHOUT CONTROL ISOLATION SYSTEM	$x_i$ (cm)	$x_i$ (cm)	WITH ACTIVE HYBRID CONTROL SYSTEM $m_d = 10\% m_i$	
				WITH PASSIVE HYBRID CONTROL SYSTEM	$\alpha/R=2.1$
B	-	14.33	9.40	8.43	5.67
1	1.29	0.42	0.28	0.27	0.18
2	1.40	0.4	0.26	0.25	0.17
3	1.22	0.3	0.20	0.19	0.13
4	1.03	0.23	0.15	0.15	0.10
5	0.73	0.15	0.10	0.10	0.07

(b) WITH P-DELTA EFFECT					
S T O R Y	WITHOUT CONTROL ISOLATION SYSTEM	$x_i$ (cm)	$x_i$ (cm)	WITH ACTIVE HYBRID CONTROL SYSTEM $m_d = 10\% m_i$	
				WITH BASE CONTROL SYSTEM	$\alpha/R=2.1$
B	-	16.76	9.91	7.53	6.847
1	1.29	0.43	0.25	0.20	0.17
2	1.40	0.41	0.23	0.20	0.17
3	1.22	0.32	0.18	0.15	0.13
4	1.03	0.25	0.14	0.12	0.10
5	0.73	0.16	0.09	0.08	0.07

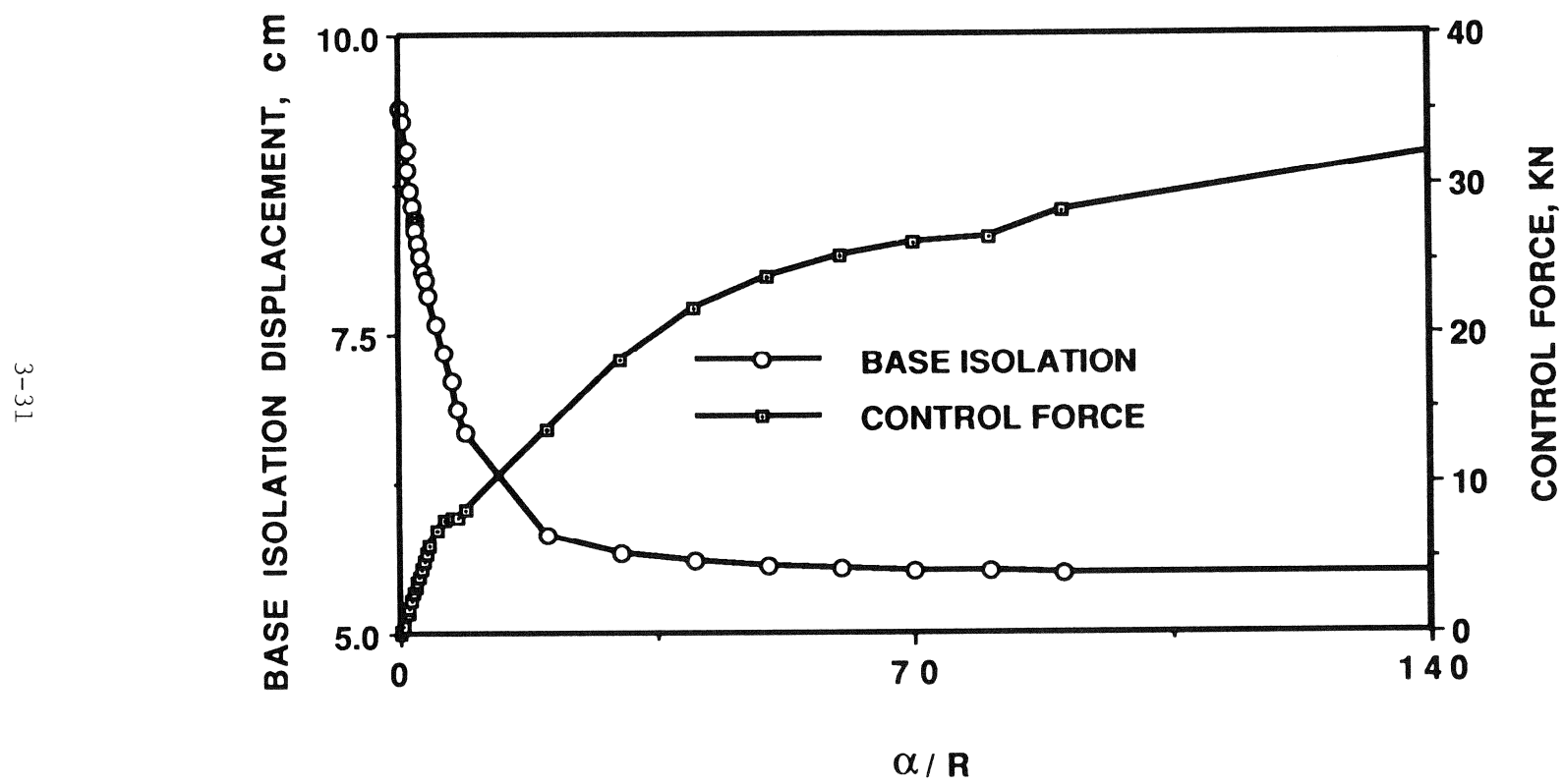


Figure 3-13: Maximum Deformation of Base Isolation System and Maximum Control Force as a Function of  $\alpha/R$ .

Instead of using the hybrid control system, consider that the building is implemented by an active mass damper on the top floor as shown in Fig. 2-1(a). The mass ratio of the damper is 10%, i.e.,  $m_d = 10\% m_i$ , and displacement and velocity sensors are installed on every floor of the building. The instantaneous optimal control law, Eq. (2.16), will be used in which the  $(12 \times 12)$  weighting matrix  $\underline{Q}$  is partitioned as shown in Eq. (3.1). The dimension of  $\underline{Q}_{21}$  and  $\underline{Q}_{22}$  matrices is  $(2 \times 6)$ . For illustrative purpose,  $R = 10^{-3}$  and elements of  $\underline{Q}_{21}$  and  $\underline{Q}_{22}$  are chosen as follows:

$$\underline{Q}_{21} = \begin{bmatrix} 30 & 60 & 60 & 60 & 500 & -0.5 \\ -3 & -5 & -9 & -10.5 & -15 & -0.052 \end{bmatrix}$$

$$\underline{Q}_{22} = \begin{bmatrix} 0.25 & 0.25 & 0.25 & 0.15 & 0.1 & -0.5 \\ -0.083 & -0.125 & -0.167 & -0.25 & -0.35 & 0.52 \end{bmatrix}$$

Time histories of all the response quantities were computed for different values of  $\alpha/R$ . Within 30 seconds of the earthquake episode, the maximum interstory deformation  $x_i$  ( $i = 1, 2, \dots, 5$ ), the maximum control force  $U$ , the maximum control force rate  $\dot{U}$  and the maximum relative displacement of the mass damper with respect to the top floor  $\bar{x}_d$  are summarized in Table 3-VI. The maximum deformation of the first story unit and the maximum control force are plotted in Fig. 3-14 as a function of  $\alpha/R$ . It is observed from Table 3-VI and Fig. 3-14 that the active control system alone is quite efficient in reducing the response of the low-rise building. A comparison between Tables 3-V and 3-VI indicates that while the active mass damper alone is capable of reducing the structural response as much as the proposed hybrid control

TABLE 3-VI: MAXIMUM STRUCTURAL RESPONSE:  
(FIVE-STORY MODEL)

ACTIVE MASS DAMPER ALONE

S T O R Y	WITHOUT CONTROL	WITH ACTIVE MASS DAMPER $m_d = 10\% m_i$		
		$\alpha/R=400$	$\alpha/R=3000$	$\alpha/R=30000$
		$m_d = 10\% m_i$ $\bar{x}_d = 8.43 \text{ cm}$	$U=23.5 \text{ kN}$ $\dot{U}=486.8 \text{ kN/sec.}$	$U=53.39 \text{ kN}$ $\dot{U}=1088.9 \text{ kN/sec}$
			$\bar{x}_d = 27.68 \text{ cm}$	$U=65.71 \text{ kN}$ $\dot{U}=1274.2 \text{ kN/sec}$
				$\bar{x}_d = 65.6 \text{ cm}$
				$\bar{x}_d = 181 \text{ cm}$
I T	$x_i$ (cm)	$x_i$ (cm)	$x_i$ (cm)	$x_i$ (cm)
1	1.29	1.26	1.16	0.42
2	1.4	1.37	1.23	0.42
3	1.22	1.19	1.03	0.31
4	1.03	1.01	0.81	0.2
5	0.73	0.71	0.51	0.11
				0.19

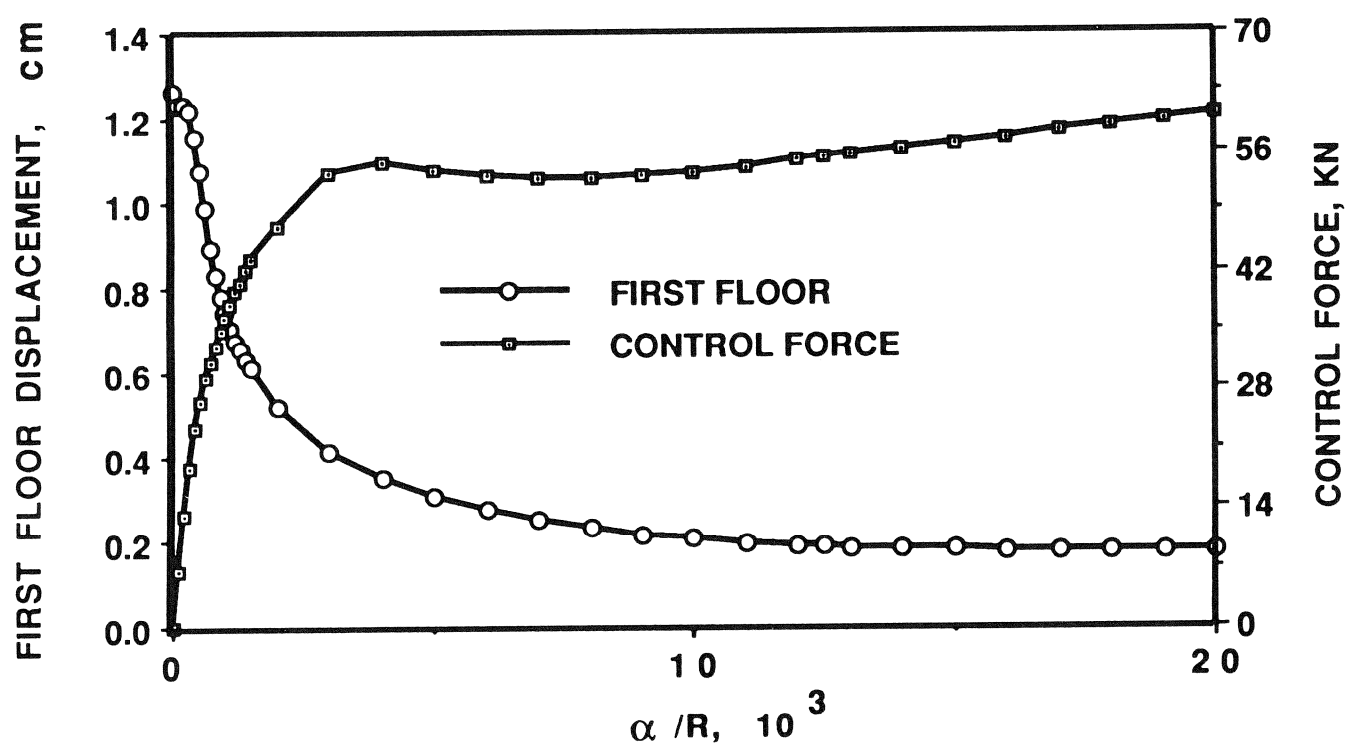


Figure 3-14: Maximum Deformation of First Story Unit and Maximum Control Force as A Function of  $\alpha/R$  (Active Mass Damper on Top Floor).

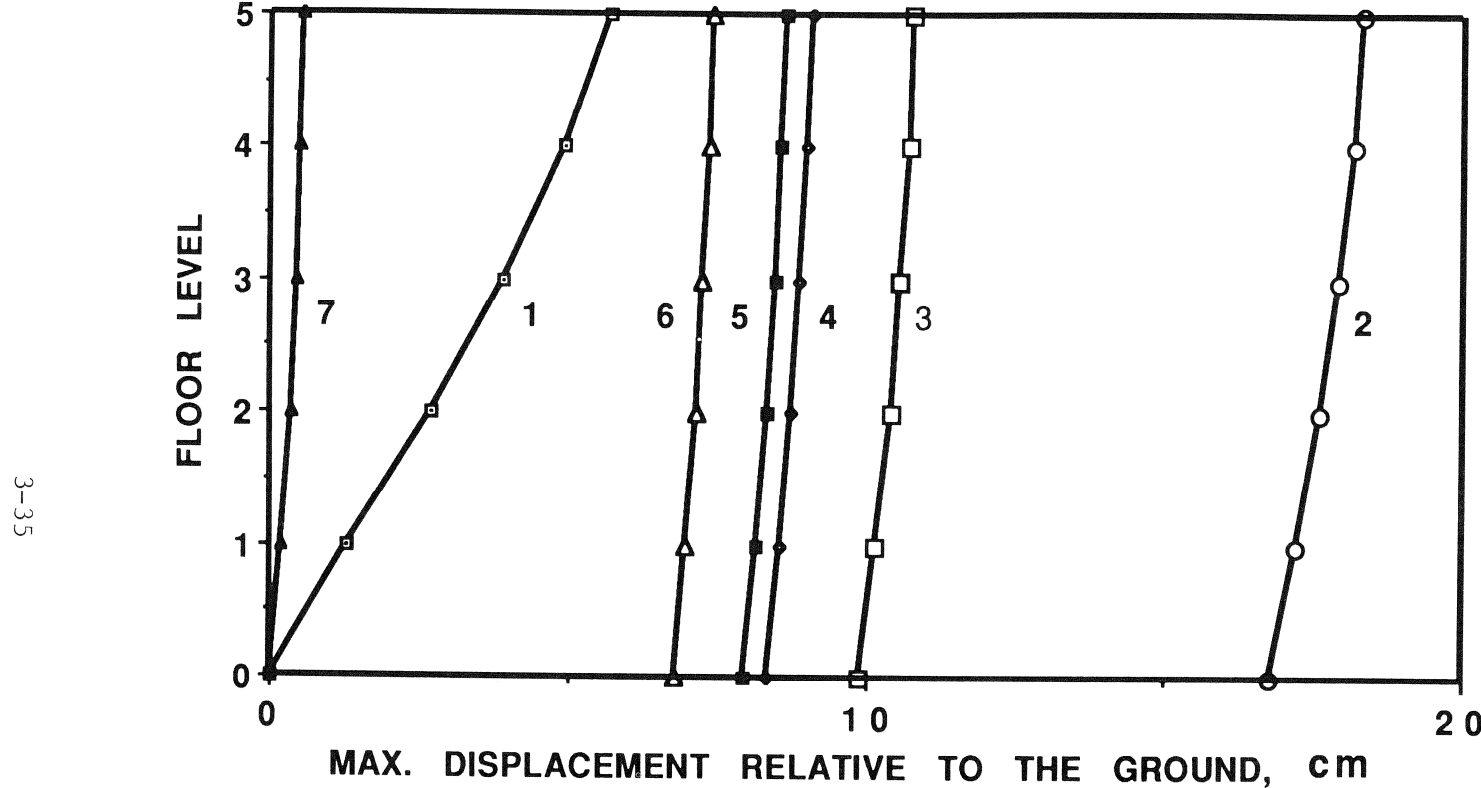


Figure 3-15: Maximum Displacement of The Building System: (1) Without Control; (2) With Base Isolation System; (3) With Passive Hybrid Control System  $m_d = 10\% m_i$ ; (4) With Passive Hybrid Control System  $m_d = 20\% m_i$ ; (5) With Passive Hybrid Control System  $m_d = 30\% m_i$ ; (6) With Active Hybrid Control System  $m_d = 10\% m_i$ ; (7) With Active Mass Damper On Top Floor  $m_d = 10\% m_i$ .

systems for low-rise buildings, the required active control force is much larger.

Within 30 seconds of the earthquake episode, the maximum displacement of the building system is plotted in Fig. 3-15 for comparison. Curve 1 in Fig. 3-15 represents the maximum response of the building without control. Curve 2 denotes the maximum response of the building with a base isolation system, where the maximum deformation of the base isolation system is indicated by the story level 0. The maximum response of the building implemented by the passive hybrid control system is shown by Curves 3-5 for the mass ratios of 10%, 20%, 30%, respectively. The result for the building implemented by the active hybrid control system is depicted by Curve 6, where the mass ratio of the damper is 10% and the maximum control force is 18.42 kN ( $\alpha/R = 30$ ). The result for the building implemented by an active mass damper on the top floor is shown by Curve 7 for the mass ratio of 10% and a maximum control force of 65.71 kN. The P-delta effect has been taken into account for all curves in Fig. 3-15. Figure 3-15 clearly demonstrates the effectiveness of the two proposed hybrid control systems.

SECTION 4  
CONCLUSIONS

Two aseismic hybrid control systems have been proposed for application to building structures against strong earthquakes. The performance of these hybrid control systems for both high-rise and low-rise buildings has been investigated and evaluated. The passive hybrid system consists of a base isolation system connected to a passive mass damper, whereas the active one consists of a base isolation system connected to an active mass damper. It is demonstrated that these hybrid control systems are very effective. It is further shown that both hybrid control systems perform better than an active mass damper alone. Another advantage of the hybrid control systems is that the mass damper, either passive or active, to be implemented at the base of the building can be easily installed through standard engineering practices.

For simplicity of evaluating the efficiency and performance of the proposed hybrid control systems, the entire structural system, including the base isolation system, is assumed to be linear elastic. In reality, many base isolation systems are either nonlinear or inelastic or both. It should be emphasized that for nonlinear or inelastic base isolation systems, the instantaneous optimal control theory developed by Yang, et al. [14,15] are applicable.



SECTION 5  
REFERENCES

1. Chan, G.K., and Kelly, J.M., "Effects of Axial Load on Elastomeric Isolation Bearings," Report No. FERC 86/12. Earthquake Engineering Research Center, University of Berkeley, Nov. 1987.
2. Constantinou, M.C., and Reinhorn, A.M., "A Working Paper on Aseismic Base Isolation," National Center For Earthquake Engineering Research, NCEER, SUNY, Buffalo, March 1988.
3. Kelly, J.M., "Aseismic Base Isolation: Review and Bibliography," Journal of Soil Dynamics and Earthquake Engr., Vol. 5, No. 3, pp. 202-216, 1986.
4. Kelly, J.M., Leitmann, G., and Soldatos, A.G., "Robust Control of Base-Isolated Structures Under Earthquake Excitation," Journal of Optimization Theory and Applications, Vol. 53, No. 2, 1987, pp. 159-180.
5. Reinhorn, A.M., and Manolis, G.D., "Current State of Knowledge on Structure Control," The Shock and Vibration Digest, Vol. 17, No. 10, 1985, pp. 35-41.
6. Reinhorn, A.M., Soong, T.T., and Yen, C.Y., "Base Isolated Structures with Active Control," Seismic Engineering, Recent Advances in Design, Analysis, Testing and Qualification Methods, Edited by Liu, T.H. and Marr, A., ASME, PVP - Vol. 127, 1987, pp. 413-419.
7. Reinhorn, A.M., Monolis, G.D., and Wen, C.Y., "Control of Structures by Coupling Rubber Isolators and Active Pulses," Proceedings of the Third U.S. National Conference on Earthquake Engineering, August 1986, Charleston, South Carolina, pp. 1899-1909.
8. Reinhorn, A.M., "Hybrid System-Combined Passive and Active Control," A Forum: Structural Applications of Protective Systems for Earthquake Hazard Mitigation," The National Center for Earthquake Engineering Research, State University of New York at Buffalo, May 19, 1987.
9. Rutenberg, A., "Simplified P-Delta Analysis for Asymmetric Structures," Journal of Structural Division, ASCE, Vol. 108, Sept. 1982, pp. 1995-2013.
10. Soong, T.T., Active Structural Control: Theory and Practice, National Center for Earthquake Engineering Research, SUNY, August 1989.
11. Wilson, E.L., and Habibullah, A., "Static and Dynamic Analysis of Multi-Story Buildings, Including P-Delta Effects," Earthquake Engineering and Structural Dynamics, Vol. 3, No. 2, 1987, pp. 289-298.
12. Yang, J.N., Akbarpour, A., and Ghaemmaghami, P., "Instantaneous Optimal Control Laws For Building Structures Under Earthquake Excitations,"

13. Yang, J.N., Akbarpour, A., and Ghaemmaghami, P., "New Optimal Control Algorithms for Structural Control," Journal of Engineering Mechanics, ASCE, Vol. 113, June 1987, pp. 1369-1386.
14. Yang, J.N., Long, F.X., and Wong, D., "Optimal Control of Nonlinear Structures," Journal of Applied Mechanics, ASCE, Vol. 55, Dec. 1988, pp. 931-938.
15. Yang, J.N., Long, F.X., and Wong, D., "Optimal Control of Nonlinear Flexible Structures," National Center For Earthquake Engineering Research, Technical Report NCEER-TR-88-0002, 1988.
16. Yang, J.N., and Soong, T.T., "Recent Advancement in Active Control of Civil Engineering Structures," Journal of Probabilistic Engineering Mechanics, Vol. 3, No. 4, Dec., 1988, pp. 179-188.
17. Yang, J.N., and Wong, D., "On Aseismic Hybrid Control System," Proceedings of 5th International Conference on Structural Safety and Reliability, ICOSAR' 89, edited by A. H-S Ang, M. Shinozuka and G.I. Schueller, ASCE, August 1989, pp. 471-478.
18. Yang, J.N., Danielians, A., and Liu, S.C., "Aseismic Hybrid Control System for Building Structures," paper accepted for publication in Journal of Engineering Mechanics, ASCE.
19. Yang, J.N., Danielians, A., and Liu, S.C., "Aseismic Hybrid Control System For Building Structures Under Strong Earthquakes," in Intelligent Structures, edited by K.P. Chong, S.C. Liu and J.C. Li, Elsevier Applied Science, 1990, pp. 179-195, Proceedings of International Workshop on Intelligent Structures, July 23-26, 1990, Taiwan, R.O.C.
20. Yao, J.T.P., "Concept of Structural Control," Journal of Structural Division, ASCE, Vol. 98, 1972, pp. 1567-1574.
21. Kelly, J.M., and Beucke, K.E., "A Friction Damped Base Isolation System with Failsafe Characteristics," Earthquake Engineering and Structural Dynamics, Vol. 11, 1983, pp. 33-56.
22. Kelly, J.M., Eridges, J.M., and Denham, C.J., "A Practical Soft Story Earthquake Isolation System," Report No. EERC 77-27, Earthquake Engineering Research Center, University of California, Berkeley, Nov. 1977.
23. Kelly, J.M., and Tsztos, D.F., "The Development of Energy-Absorbing Devices for Aseismic Base Isolation Systems," Report No. EERC 78/01, Earthquake Engineering Research Center, University of Berkeley, Jan. 1978.

**NATIONAL CENTER FOR EARTHQUAKE ENGINEERING RESEARCH**  
**LIST OF TECHNICAL REPORTS**

The National Center for Earthquake Engineering Research (NCEER) publishes technical reports on a variety of subjects related to earthquake engineering written by authors funded through NCEER. These reports are available from both NCEER's Publications Department and the National Technical Information Service (NTIS). Requests for reports should be directed to the Publications Department, National Center for Earthquake Engineering Research, State University of New York at Buffalo, Red Jacket Quadrangle, Buffalo, New York 14261. Reports can also be requested through NTIS, 5285 Port Royal Road, Springfield, Virginia 22161. NTIS accession numbers are shown in parenthesis, if available.

- NCEER-87-0001 "First-Year Program in Research, Education and Technology Transfer," 3/5/87, (PB88-134275/AS).
- NCEER-87-0002 "Experimental Evaluation of Instantaneous Optimal Algorithms for Structural Control," by R.C. Lin, T.T. Soong and A.M. Reinhorn, 4/20/87, (PB88-134341/AS).
- NCEER-87-0003 "Experimentation Using the Earthquake Simulation Facilities at University at Buffalo," by A.M. Reinhorn and R.L. Ketter, to be published.
- NCEER-87-0004 "The System Characteristics and Performance of a Shaking Table," by J.S. Hwang, K.C. Chang and G.C. Lee, 6/1/87, (PB88-134259/AS). This report is available only through NTIS (see address given above).
- NCEER-87-0005 "A Finite Element Formulation for Nonlinear Viscoplastic Material Using a Q Model," by O. Gyebi and G. Dasgupta, 11/2/87, (PB88-213764/AS).
- NCEER-87-0006 "Symbolic Manipulation Program (SMP) - Algebraic Codes for Two and Three Dimensional Finite Element Formulations," by X. Lee and G. Dasgupta, 11/9/87, (PB88-219522/AS).
- NCEER-87-0007 "Instantaneous Optimal Control Laws for Tall Buildings Under Seismic Excitations," by J.N. Yang, A. Akbarpour and P. Ghoshmaghani, 6/10/87, (PB88-134333/AS).
- NCEER-87-0008 "IDARC: Inelastic Damage Analysis of Reinforced Concrete Frame - Shear-Wall Structures," by Y.J. Park, A.M. Reinhorn and S.K. Kunmath, 7/20/87, (PB88-134325/AS).
- NCEER-87-0009 "Liquefaction Potential for New York State: A Preliminary Report on Sites in Manhattan and Buffalo," by M. Budhu, V. Vijayakumar, R.F. Giese and L. Baumgras, 8/31/87, (PB88-163704/AS). This report is available only through NTIS (see address given above).
- NCEER-87-0010 "Vertical and Torsional Vibration of Foundations in Inhomogeneous Media," by A.S. Veletsos and K.W. Dotson, 6/1/87, (PB88-134291/AS).
- NCEER-87-0011 "Seismic Probabilistic Risk Assessment and Seismic Margins Studies for Nuclear Power Plants," by Howard H.M. Hwang, 6/15/87, (PB88-134267/AS).
- NCEER-87-0012 "Parametric Studies of Frequency Response of Secondary Systems Under Ground-Acceleration Excitations," by Y. Yong and Y.K. Lin, 6/10/87, (PB88-134309/AS).
- NCEER-87-0013 "Frequency Response of Secondary Systems Under Seismic Excitation," by J.A. HoLung, J. Cai and Y.K. Lin, 7/31/87, (PB88-134317/AS).
- NCEER-87-0014 "Modelling Earthquake Ground Motions in Seismically Active Regions Using Parametric Time Series Methods," by G.W. Ellis and A.S. Cakmak, 8/25/87, (PB88-134283/AS).
- NCEER-87-0015 "Detection and Assessment of Seismic Structural Damage," by E. DiPasquale and A.S. Cakmak, 8/25/87, (PB88-163712/AS).
- NCEER-87-0016 "Pipeline Experiment at Parkfield, California," by J. Isenberg and E. Richardson, 9/15/87, (PB88-163720/AS). This report is available only through NTIS (see address given above).

- NCEER-87-0017 "Digital Simulation of Seismic Ground Motion," by M. Shinozuka, G. Deodatis and T. Harada, 8/31/87, (PB88-155197/AS). This report is available only through NTIS (see address given above).
- NCEER-87-0018 "Practical Considerations for Structural Control: System Uncertainty, System Time Delay and Truncation of Small Control Forces," J.N. Yang and A. Akbarpour, 8/10/87, (PB88-163738/AS).
- NCEER-87-0019 "Modal Analysis of Nonclassically Damped Structural Systems Using Canonical Transformation," by J.N. Yang, S. Sarkani and F.X. Long, 9/27/87, (PB88-187851/AS).
- NCEER-87-0020 "A Nonstationary Solution in Random Vibration Theory," by J.R. Red-Horse and P.D. Spanos, 11/3/87, (PB88-163746/AS).
- NCEER-87-0021 "Horizontal Impedances for Radially Inhomogeneous Viscoelastic Soil Layers," by A.S. Veletos and K.W. Dotson, 10/15/87, (PB88-150859/AS).
- NCEER-87-0022 "Seismic Damage Assessment of Reinforced Concrete Members," by Y.S. Chung, C. Meyer and M. Shinozuka, 10/9/87, (PB88-150867/AS). This report is available only through NTIS (see address given above).
- NCEER-87-0023 "Active Structural Control in Civil Engineering," by T.T. Soong, 11/11/87, (PB88-187778/AS).
- NCEER-87-0024 "Vertical and Torsional Impedances for Radially Inhomogeneous Viscoelastic Soil Layers," by K.W. Dotson and A.S. Veletos, 12/87, (PB88-187786/AS).
- NCEER-87-0025 "Proceedings from the Symposium on Seismic Hazards, Ground Motions, Soil-Liquefaction and Engineering Practice in Eastern North America," October 20-22, 1987, edited by K.H. Jacob, 12/87, (PB88-188115/AS).
- NCEER-87-0026 "Report on the Whittier-Narrows, California, Earthquake of October 1, 1987," by J. Pantelic and A. Reinhorn, 11/87, (PB88-187752/AS). This report is available only through NTIS (see address given above).
- NCEER-87-0027 "Design of a Modular Program for Transient Nonlinear Analysis of Large 3-D Building Structures," by S. Srivastav and J.F. Abel, 12/30/87, (PB88-187950/AS).
- NCEER-87-0028 "Second-Year Program in Research, Education and Technology Transfer," 3/8/88, (PB88-219480/AS).
- NCEER-87-0029 "Workshop on Seismic Computer Analysis and Design of Buildings With Interactive Graphics," by W. McGuire, J.F. Abel and C.H. Conley, 1/18/88, (PB88-187760/AS).
- NCEER-88-0002 "Optimal Control of Nonlinear Flexible Structures," by J.N. Yang, F.X. Long and D. Wong, 1/22/88, (PB88-213772/AS).
- NCEER-88-0003 "Substructuring Techniques in the Time Domain for Primary-Secondary Structural Systems," by G.D. Manolis and G. Juhn, 2/10/88, (PB88-213780/AS).
- NCEER-88-0004 "Iterative Seismic Analysis of Primary-Secondary Systems," by A. Singhal, L.D. Lutes and P.D. Spanos, 2/23/88, (PB88-213798/AS).
- NCEER-88-0005 "Stochastic Finite Element Expansion for Random Media," by P.D. Spanos and R. Ghanem, 3/14/88, (PB88-213806/AS).
- NCEER-88-0006 "Combining Structural Optimization and Structural Control," by F.Y. Cheng and C.P. Pantelides, 1/10/88, (PB88-213814/AS).
- NCEER-88-0007 "Seismic Performance Assessment of Code-Designed Structures," by H.H-M. Hwang, J-W. Jaw and H.J. Shau, 3/20/88, (PB88-219423/AS).

NCEER-88-0008	"Reliability Analysis of Code-Designed Structures Under Natural Hazards," by H.H-M. Hwang, H. Ushiba and M. Shinouzuka, 2/29/88, (PB88-229471/AS).
NCEER-88-0009	"Seismic Fragility Analysis of Shear Wall Structures," by J-W Jaw and H.H-M. Hwang, 4/30/88, (PB89-102867/AS).
NCEER-88-0010	"Base Isolation of a Multi-Story Building Under a Harmonic Ground Motion - A Comparison of Performances of Various Systems," by F-G Fan, G. Ahmadi and I.G. Tadjbakish, 5/18/88, (PB89-122238/AS).
NCEER-88-0011	"Seismic Floor Response Spectra for a Combined System by Green's Functions," by F.M. Lavelle, L.A. Bergman and P.D. Spanos, 5/1/88, (PB89-102875/AS).
NCEER-88-0012	"A New Solution Technique for Randomly Excited Hysteretic Structures," by G.Q. Cai and Y.K. Lin, 5/16/88, (PB89-102883/AS).
NCEER-88-0013	"A Study of Radiation Damping and Soil-Structure Interaction Effects in the Centrifuge," by K. Weissman, supervised by J.H. Prevost, 5/24/88, (PB89-144703/AS).
NCEER-88-0014	"Parameter Identification and Implementation of a Kinematic Plasticity Model for Frictional Soils," by J.H. Prevost and D.V. Griffiths, to be published.
NCEER-88-0015	"Two- and Three- Dimensional Dynamic Finite Element Analyses of the Long Valley Dam," by D.V. Griffiths and J.H. Prevost, 6/17/88, (PB89-144711/AS).
NCEER-88-0016	"Damage Assessment of Reinforced Concrete Structures in Eastern United States," by A.M. Reinhorn, M.J. Seidel, S.K. Kunath and Y.J. Park, 6/15/88, (PB89-122220/AS).
NCEER-88-0017	"Dynamic Compliance of Vertically Loaded Strip Foundations in Multilayered Viscoelastic Soils," by S. Ahmad and A.S.M. Israil, 6/17/88, (PB89-102891/AS).
NCEER-88-0018	"An Experimental Study of Seismic Structural Response With Added Viscoelastic Dampers," by R.C. Lin, Z. Liang, T.T. Soong and R.H. Zhang, 6/30/88, (PB89-122212/AS).
NCEER-88-0019	"Experimental Investigation of Primary - Secondary System Interaction," by G.D. Manolis, G. Juhn and A.M. Reinhorn, 5/27/88, (PB89-122204/AS).
NCEER-88-0020	"A Response Spectrum Approach For Analysis of Nonclassically Damped Structures," by J.N. Yang, S. Sarkani and F.X. Long, 4/22/88, (PB89-102909/AS).
NCEER-88-0021	"Seismic Interaction of Structures and Soils: Stochastic Approach," by A.S. Veltos and A.M. Prasad, 7/21/88, (PB89-122196/AS).
NCEER-88-0022	"Identification of the Serviceability Limit State and Detection of Seismic Structural Damage," by E. DiPasquale and A.S. Cakmak, 6/15/88, (PB89-122188/AS).
NCEER-88-0023	"Multi-Hazard Risk Analysis: Case of a Simple Offshore Structure," by B.K. Bhartia and E.H. Vanmarcke, 7/21/88, (PB89-145213/AS).
NCEER-88-0024	"Automated Seismic Design of Reinforced Concrete Buildings," by Y.S. Chung, C. Meyer and M. Shinouzuka, 7/5/88, (PB89-122170/AS).
NCEER-88-0025	"Experimental Study of Active Control of MDOF Structures Under Seismic Excitations," by L.L. Chung, R.C. Lin, T.T. Soong and A.M. Reinhorn, 7/10/88, (PB89-122600/AS).
NCEER-88-0026	"Earthquake Simulation Tests of a Low-Rise Metal Structure," by J.S. Hwang, K.C. Chang, G.C. Lee and R.L. Ketter, 8/1/88, (PB89-102917/AS).
NCEER-88-0027	"Systems Study of Urban Response and Reconstruction Due to Catastrophic Earthquakes," by F. Kozin and H.K. Zhou, 9/22/88, (PB90-162348/AS).

- NCEER-88-0028 "Seismic Fragility Analysis of Plane Frame Structures," by H.H-M. Hwang and Y.K. Low, 7/31/88, (PB89-131445/AS).
- NCEER-88-0029 "Response Analysis of Stochastic Structures," by A. Kardara, C. Bucher and M. Shinozuka, 9/22/88, (PB89-174429/AS).
- NCEER-88-0030 "Nonnormal Accelerations Due to Yielding in a Primary Structure," by D.C.K. Chen and L.D. Lutes, 9/19/88, (PB89-131437/AS).
- NCEER-88-0031 "Design Approaches for Soil-Structure Interaction," by A.S. Veletsos, A.M. Prasad and Y. Tang, 12/30/88, (PB89-174437/AS).
- NCEER-88-0032 "A Re-evaluation of Design Spectra for Seismic Damage Control," by C.J. Turkstra and A.G. Tallin, 11/7/88, (PB89-145221/AS).
- NCEER-88-0033 "The Behavior and Design of Noncontact Lap Splices Subjected to Repeated Inelastic Tensile Loading," by V.E. Sagan, P. Gergely and R.N. White, 12/8/88, (PB89-163737/AS).
- NCEER-88-0034 "Seismic Response of Pile Foundations," by S.M. Mamoon, P.K. Banerjee and S. Ahmad, 11/1/88, (PB89-145239/AS).
- NCEER-88-0035 "Modeling of R/C Building Structures With Flexible Floor Diaphragms (IDARC2)," by A.M. Reinhard, S.K. Kurmath and N. Panahshahi, 9/7/88, (PB89-207153/AS).
- NCEER-88-0036 "Solution of the Dam-Reservoir Interaction Problem Using a Combination of FEM, BEM with Particular Integrals, Modal Analysis, and Substructuring," by C-S. Tsai, G.C. Lee and R.L. Ketter, 12/31/88, (PB89-207146/AS).
- NCEER-88-0037 "Optimal Placement of Actuators for Structural Control," by F.Y. Cheng and C.P. Pantelides, 8/15/88, (PB89-162846/AS).
- NCEER-88-0038 "Teflon Bearings in Aseismic Base Isolation: Experimental Studies and Mathematical Modeling," by A. Mokha, M.C. Constantinou and A.M. Reinhard, 12/5/88, (PB89-218457/AS).
- NCEER-88-0039 "Seismic Behavior of Flat Slab High-Rise Buildings in the New York City Area," by P. Weidlinger and M. Ettouney, 10/15/88, (PB90-145681/AS).
- NCEER-88-0040 "Evaluation of the Earthquake Resistance of Existing Buildings in New York City," by P. Weidlinger and M. Ettouney, 10/15/88, to be published.
- NCEER-88-0041 "Small-Scale Modeling Techniques for Reinforced Concrete Structures Subjected to Seismic Loads," by W. Kim, A. El-Attar and R.N. White, 11/22/88, (PB89-189625/AS).
- NCEER-88-0042 "Modeling Strong Ground Motion from Multiple Event Earthquakes," by G.W. Ellis and A.S. Cakmak, 10/15/88, (PB89-174445/AS).
- NCEER-88-0043 "Nonstationary Models of Seismic Ground Acceleration," by M. Grigoriu, S.E. Ruiz and E. Rosenblueth, 7/15/88, (PB89-189617/AS).
- NCEER-88-0044 "SARCF User's Guide: Seismic Analysis of Reinforced Concrete Frames," by Y.S. Chung, C. Meyer and M. Shinozuka, 11/9/88, (PB89-174452/AS).
- NCEER-88-0045 "First Expert Panel Meeting on Disaster Research and Planning," edited by J. Pantelic and J. Stoyle, 9/15/88, (PB89-174460/AS).
- NCEER-88-0046 "Preliminary Studies of the Effect of Degrading Infill Walls on the Nonlinear Seismic Response of Steel Frames," by C.Z. Chrysostomou, P. Gergely and J.F. Abel, 12/19/88, (PB89-208383/AS).

NCEER-88-0047	"Reinforced Concrete Frame Component Testing Facility - Design, Construction, Instrumentation and Operation," by S.P. Pessiki, C. Conley, T. Bond, P. Gergely and R.N. White, 12/16/88, (PB89-174478/AS).
NCEER-89-0001	"Effects of Protective Cushion and Soil Compliancy on the Response of Equipment Within a Seismically Excited Building," by J.A. HoLung, 2/16/89, (PB89-207179/AS).
NCEER-89-0002	"Statistical Evaluation of Response Modification Factors for Reinforced Concrete Structures," by H.H.-M. Hwang and J.-W. Jaw, 2/17/89, (PB89-207187/AS).
NCEER-89-0003	"Hysteretic Columns Under Random Excitation," by G-Q. Cai and Y.K. Lin, 1/9/89, (PB89-196513/AS).
NCEER-89-0004	"Experimental Study of 'Elephant Foot Bulge' Instability of Thin-Walled Metal Tanks," by Z-H. Jia and R.L. Ketter, 2/22/89, (PB89-207195/AS).
NCEER-89-0005	"Experiment on Performance of Buried Pipelines Across San Andreas Fault," by J. Isenberg, E. Richardson and T.D. O'Rourke, 3/10/89, (PB89-218440/AS).
NCEER-89-0006	"A Knowledge-Based Approach to Structural Design of Earthquake-Resistant Buildings," by M. Subramani, P. Gergely, C.H. Conley, J.F. Abel and A.H. Zaghw, 1/15/89, (PB89-218465/AS).
NCEER-89-0007	"Liquefaction Hazards and Their Effects on Buried Pipelines," by T.D. O'Rourke and P.A. Lane, 2/1/89, (PB89-218481).
NCEER-89-0008	"Fundamentals of System Identification in Structural Dynamics," by H. Imai, C-B. Yun, O. Manyama and M. Shinozuka, 1/26/89, (PB89-207211/AS).
NCEER-89-0009	"Effects of the 1985 Michoacan Earthquake on Water Systems and Other Buried Lifelines in Mexico," by A.G. Ayala and M.J. O'Rourke, 3/8/89, (PB89-207229/AS).
NCEER-89-R010	"NCEER Bibliography of Earthquake Education Materials," by K.E.K. Ross, Second Revision, 9/1/89, (PB90-123532/AS).
NCEER-89-0011	"Inelastic Three-Dimensional Response Analysis of Reinforced Concrete Building Structures (IDARC-3D), Part I - Modeling," by S.K. Kunmath and A.M. Reinhorn, 4/17/89, (PB90-114612/AS).
NCEER-89-0012	"Recommended Modifications to ATC-14," by C.D. Poland and J.O. Malley, 4/12/89, (PB90-108648/AS).
NCEER-89-0013	"Repair and Strengthening of Beam-to-Column Connections Subjected to Earthquake Loading," by M. Corazao and A.J. Durran, 2/28/89, (PB90-109885/AS).
NCEER-89-0014	"Program EXKAL2 for Identification of Structural Dynamic Systems," by O. Maruyama, C-B. Yun, M. Hoshiya and M. Shinozuka, 5/19/89, (PB90-109877/AS).
NCEER-89-0015	"Response of Frames With Bolted Semi-Rigid Connections, Part I - Experimental Study and Analytical Predictions," by P.J. DiCorso, A.M. Reinhorn, J.R. Dickerson, J.B. Radzimski and W.L. Harper, 6/1/89, to be published.
NCEER-89-0016	"ARMA Monte Carlo Simulation in Probabilistic Structural Analysis," by P.D. Spanos and M.P. Mignolet, 7/10/89, (PB90-109893/AS).
NCEER-89-P017	"Preliminary Proceedings from the Conference on Disaster Preparedness - The Place of Earthquake Education in Our Schools," Edited by K.E.K. Ross, 6/23/89.
NCEER-89-0017	"Proceedings from the Conference on Disaster Preparedness - The Place of Earthquake Education in Our Schools," Edited by K.E.K. Ross, 12/31/89, (PB90-207895).

- NCEER-89-0018 "Multidimensional Models of Hysteretic Material Behavior for Vibration Analysis of Shape Memory Energy Absorbing Devices, by E.J. Graesser and F.A. Cozzarelli, 6/7/89, (PB90-164146/AS).
- NCEER-89-0019 "Nonlinear Dynamic Analysis of Three-Dimensional Base Isolated Structures (3D-BASIS)," by S. Nagarajaiah, A.M. Reinhard and M.C. Constantinou, 8/3/89, (PB90-161936/AS).
- NCEER-89-0020 "Structural Control Considering Time-Rate of Control Forces and Control Rate Constraints," by F.Y. Cheng and C.P. Pantelides, 8/3/89, (PB90-120445/AS).
- NCEER-89-0021 "Subsurface Conditions of Memphis and Shelby County," by K.W. Ng, T-S. Chang and H-H.M. Hwang, 7/26/89, (PB90-120437/AS).
- NCEER-89-0022 "Seismic Wave Propagation Effects on Straight Jointed Buried Pipelines," by K. Elmadi and M.J. O'Rourke, 8/24/89, (PB90-162322/AS).
- NCEER-89-0023 "Workshop on Serviceability Analysis of Water Delivery Systems," edited by M. Grigoriu, 3/6/89, (PB90-127424/AS).
- NCEER-89-0024 "Shaking Table Study of a 1/5 Scale Steel Frame Composed of Tapered Members," by K.C. Chang, J.S. Hwang and G.C. Lee, 9/18/89, (PB90-160169/AS).
- NCEER-89-0025 "DYNA1D: A Computer Program for Nonlinear Seismic Site Response Analysis - Technical Documentation," by Jean H. Prevost, 9/14/89, (PB90-161944/AS).
- NCEER-89-0026 "1:4 Scale Model Studies of Active Tendon Systems and Active Mass Dampers for Aseismic Protection," by A.M. Reinhorn, T.T. Soong, R.C. Lin, Y.P. Yang, Y. Fukao, H. Abe and M. Nakai, 9/15/89, (PB90-173246/AS).
- NCEER-89-0027 "Scattering of Waves by Inclusions in a Nonhomogeneous Elastic Half Space Solved by Boundary Element Methods," by P.K. Hadley, A. Askar and A.S. Cakmak, 6/15/89, (PB90-145699/AS).
- NCEER-89-0028 "Statistical Evaluation of Deflection Amplification Factors for Reinforced Concrete Structures," by H.H.M. Hwang, J.-W. Jaw and A.L. Ch'ng, 8/31/89, (PB90-164633/AS).
- NCEER-89-0029 "Bedrock Accelerations in Memphis Area Due to Large New Madrid Earthquakes," by H.H.M. Hwang, C.H.S. Chen and G. Yu, 11/7/89, (PB90-162330/AS).
- NCEER-89-0030 "Seismic Behavior and Response Sensitivity of Secondary Structural Systems," by Y.Q. Chen and T.T. Soong, 10/23/89, (PB90-164658/AS).
- NCEER-89-0031 "Random Vibration and Reliability Analysis of Primary-Secondary Structural Systems," by Y. Ibrahim, M. Grigoriu and T.T. Soong, 11/10/89, (PB90-161951/AS).
- NCEER-89-0032 "Proceedings from the Second U.S. - Japan Workshop on Liquefaction, Large Ground Deformation and Their Effects on Lifelines, September 26-29, 1989," Edited by T.D. O'Rourke and M. Hamada, 12/1/89, (PB90-209388/AS).
- NCEER-89-0033 "Deterministic Model for Seismic Damage Evaluation of Reinforced Concrete Structures," by J.M. Bracci, A.M. Reinhard, J.B. Mander and S.K. Kunrath, 9/27/89.
- NCEER-89-0034 "On the Relation Between Local and Global Damage Indices," by E. DiPasquale and A.S. Cakmak, 8/15/89, (PB90-173865).
- NCEER-89-0035 "Cyclic Undrained Behavior of Nonplastic and Low Plasticity Soils," by A.J. Walker and H.E. Stewart, 7/26/89, (PB90-183518/AS).
- NCEER-89-0036 "Liquefaction Potential of Surficial Deposits in the City of Buffalo, New York," by M. Budhu, R. Giese and L. Baumgrass, 1/17/89, (PB90-208455/AS).

- NCEER-89-0037 "A Deterministic Assessment of Effects of Ground Motion Incoherence," by A.S. Veletsos and Y. Tang, 7/15/89, (PB90-164294/AS).
- NCEER-89-0038 "Workshop on Ground Motion Parameters for Seismic Hazard Mapping," July 17-18, 1989, edited by R.V. Whitman, 12/1/89, (PB90-173923/AS).
- NCEER-89-0039 "Seismic Effects on Elevated Transit Lines of the New York City Transit Authority," by C.J. Costantino, C.A. Miller and E. Heymsfield, 12/26/89, (PB90-207887/AS).
- NCEER-89-0040 "Centrifugal Modeling of Dynamic Soil-Structure Interaction," by K. Weissman, Supervised by J.H. Prevost, 5/10/89, (PB90-207879/AS).
- NCEER-89-0041 "Linearized Identification of Buildings With Cores for Seismic Vulnerability Assessment," by I-K. Ho and A.E. Aktan, 11/1/89.
- NCEER-90-0001 "Geotechnical and Lifeline Aspects of the October 17, 1989 Loma Prieta Earthquake in San Francisco," by T.D. O'Rourke, H.E. Stewart, F.T. Blackburn and T.S. Dickerman, 1/90, (PB90-208596/AS).
- NCEER-90-0002 "Nonnormal Secondary Response Due to Yielding in a Primary Structure," by D.C.K. Chen and L.D. Lutes, 2/28/90.
- NCEER-90-0003 "Earthquake Education Materials for Grades K-12," by K.E.K. Ross, 4/16/90.
- NCEER-90-0004 "Catalog of Strong Motion Stations in Eastern North America," by R.W. Busby, 4/3/90.
- NCEER-90-0005 "NCEER Strong-Motion Data Base: A User Manual for the GeoBase Release (Version 1.0 for the Sun3)," by P. Friberg and K. Jacob, 3/31/90.
- NCEER-90-0006 "Seismic Hazard Along a Crude Oil Pipeline in the Event of an 1811-1812 Type New Madrid Earthquake," by H.H.M. Hwang and C-H.S. Chen, 4/16/90.
- NCEER-90-0007 "Site-Specific Response Spectra for Memphis Sheahan Pumping Station," by H.H.M. Hwang and C.S. Lee, 5/15/90.
- NCEER-90-0008 "Pilot Study on Seismic Vulnerability of Crude Oil Transmission Systems," by T. Ariman, R. Dobry, M. Grigoriu, F. Kozin, M. O'Rourke, T. O'Rourke and M. Shinouzuka, 5/25/90.
- NCEER-90-0009 "A Program to Generate Site Dependent Time Histories: EQGEN," by G.W. Ellis, M. Srinivasan and A.S. Cakmak, 1/30/90.
- NCEER-90-0010 "Active Isolation for Seismic Protection of Operating Rooms," by M.E. Talbot, Supervised by M. Shinouzuka, 6/8/90.
- NCEER-90-0011 "Program LINEARID for Identification of Linear Structural Dynamic Systems," by C-B. Yun and M. Shinouzuka, 6/25/90.
- NCEER-90-0012 "Two-Dimensional Two-Phase Elasto-Plastic Seismic Response of Earth Dams," by A.N. Yiagos, Supervised by J.H. Prevost, 6/20/90.
- NCEER-90-0013 "Secondary Systems in Base-Isolated Structures: Experimental Investigation, Stochastic Response and Stochastic Sensitivity," by G.D. Manolis, G. Juhn, M.C. Constantinou and A.M. Reinhard, 7/1/90.
- NCEER-90-0014 "Seismic Behavior of Lightly-Reinforced Concrete Column and Beam-Column Joint Details," by S.P. Pessiki, C.H. Conley, P. Gergely and R.N. White, 8/22/90.
- NCEER-90-0015 "Two Hybrid Control Systems for Building Structures Under Strong Earthquakes," by J.N. Yang and A. Danielians, 6/29/90.





National Center for Earthquake Engineering Research  
State University of New York at Buffalo

14